Czech Technical University in Prague
Faculty of Electrical Engineering
Department of Control Engineering

master's thesis

Propagation of elastic waves through locally periodic structures

Hanna Chaika

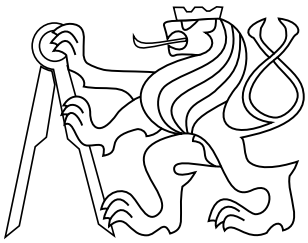

Supervisor: doc. Dr. Ing. Michal Bednarik

January 2018

České vysoké učení technické v Praze
Fakulta elektrotechnická

katedra řídicí techniky

ZADÁNÍ DIPLOMOVÉ PRÁCE

Student: **Chaika Hanna**

Studijní program: Kybernetika a robotika
Obor: Systémy a řízení

Název tématu: **Šíření elastických vln lokálně periodickými strukturami**

Pokyny pro vypracování:

Prozkoumejte elastické vlny šířící se skrz disperzní zónou využívající prostorově neuniformní závislosti hustoty a elastických vlastností uvažovaných materiálů, což nám umožňuje řídit odrazy a průchody akustických vlny v dané spektrální oblasti. Jako nelokální disperzní zóny předpokládáme použít prostorově omezené oblasti s funkčně proměnnými materiálovými vlastnostmi. Použijte lokálně periodické struktury založené na výše zmíněných nelokálních disperzních zónách, protože i relativně malý počet opakujících se nelokálních disperzních zón vykazuje téměř nulový přenos akustické energie v některých frekvenčních pásmech.

Seznam odborné literatury:

[1] David J. Griffiths and Carl A. Steinke, "Waves in locally periodic media", Am. J. Phys. 69 (2), 2001.
[2] Zhuangqi Cao and Cheng Yin,"Advances in One-Dimensional Wave Mechanics", Springer, 2014.
[3] Peter Markoš and Costas M. Soukoulis, "Wave Propagation - From Electrons to Photonic Crystals and Left-Handed Materials", Princeton University Press, 2008.

Vedoucí: doc. Dr. Ing. Michal Bednařík

Platnost zadání: do konce letního semestru 2017/2018

L.S.

prof. Ing. Michael Šebek, DrSc.
vedoucí katedry

prof. Ing. Pavel Ripka, CSc.
děkan

V Praze, dne 30. 1. 2017

Acknowledgement

I would like to thank my family, friends and colleagues for their support and, of course, I would like to express the gratitude to my supervisor for his immense knowledge and patience.

Declaration

I declare that I completed the presented thesis independently and that all used sources are quoted in accordance with the Methodological Instructions that cover the ethical principles for writing an academic thesis.

In Prague on ....
Signature

Abstrakt

Diplomová práce se zabývá šířením podélných elastických vln lokálně periodickými strukturami vybuzenými harmonickou silou. Stejně jako v mnoha periodických systémech šíření elastických vln periodickými strukturami vede ke kmitočtovým pásmovým propadům, tj. k širokým kmitočtovým oblastem, kterými se dopadající vlna nešíří. Materiál lokálně periodických struktur vykazuje nestejnorodou závislost hustoty a elastických parametrů. Vlnovod se skládá z *buňek*, přičemž jsou uvažovány buňky s nestejnorodým průřezem, různými materiály a rovněž materiálem, který mění své elastické vlastnosti lineárně v závislosti na prostorové souřadnici. Odpovídající modelová rovnice je odvozena. Ke studiu elastických vln procházejících nehomogenní oblastí je použita metoda využívající přenosové matice. Výpočet přenosových matic je proveden nalézením obecného řešení v intervalu obsahujícím dva regulární singulární body. Na základě přenosových matic je studován vliv vybraných parametrů na spektrum koeficientu přenosu. Výpočet koeficientu přenosu lokálně periodické struktury pro N opakujících se buněk se počítá pomocí Chebyshevových polynomů.

Klíčová slova

Přenosová matice; koeficient transmise; elastické vlny; nestejnorodá hustota a elastické parametry materiálů; lokálně periodické struktury.

Abstract

This master thesis presents the propagation of the longitudinal elastic waves through the locally periodic structures excited by a harmonic force. As in many periodic systems, elastic wave propagation through the periodic structures results in the frequency band gaps, or large ranges of the incident wave frequency over which no wave is transmitted. The material of the locally periodic structures has non-uniform profile of the mass density and elastic properties. *Cells* with non-uniform cross-section, different materials and linearly graded material, constituting the solid rod, are considered. The corresponding model equation is derived. The transfer matrix method is applied to study the elastic waves passing through the inhomogeneous domain. The calculation of the transfer matrices goes through the evaluation of the general solution in the interval containing two regular singular points. Based on the transfer matrices the influence of the chosen parameter values on the transmission coefficient spectrum is studied. The transmission coefficient calculation of locally periodic structures for N repeating cells is calculated with the help of the Chebyshev polynomials.

Keywords

Transfer matrix; transmission coefficient; elastic waves; non-uniform mass density and elastic properties of materials; locally periodic structures.

Contents

Abbreviations

Latin capital letters

A	cross section
$A(x)$	non-uniform cross section
A, B	cell regions
$\mathcal{A}$, $\mathcal{B}$, $\mathcal{C}$, $\mathcal{D}$	complex amplitudes
C_1, C_2	complex integration constants
C_3, C_4	complex integration constants
$E(x)$	non-uniform Young's modulus
E, E_0	constant Young's moduli
F	force
$\mathcal{F}$, $\mathcal{G}$	complex amplitudes
$\mathrm{J_n}$	Bessel function of the 1st kind of order n
K	dimensionless wave number
$\mathbf{M}$	transfer matrix
N	number of cells
$\mathbf{P}$	*shifted* transfer matrix
$R(s)$	dimensionless radius of the solid rod
$S(s)$	dimensionless cross-section
$\mathbf{S}$	scattering matrix
$\mathcal{T}$	transmission coefficient
$\mathcal{T}_N$	transmission coefficient for N cells
$U_N(x)$	Chebyshev polynomial of the second kind
$\hat{U}(s)$	dimensionless amplitude of local displacement
V	volume fraction
$\mathrm{Y_n}$	Bessel function of the 2nd kind of order n

Latin lowercase letters

a	$=(E_{\mathrm{II}} - E_{\mathrm{I}})/E_{\mathrm{I}}$, constant
$arg_a(s)$	$= 2K_{\mathrm{A}}\sqrt{1+as}/a$, expression
$arg_b(s)$	$= 2K_{\mathrm{B}}\sqrt{1-bs}/b$, expression
b	$=(E_{\mathrm{II}} - E_{\mathrm{I}})/E_{\mathrm{II}}$, constant
c_L	$= \sqrt{E(s)/\rho_0}$, wave speed in media with non-uniform Young's modulus
c_{L0}	wave speed in media with constant characteristics
f	frequency
l	length between the closest sides of neighboring cells
ℓ	characteristic length
m	the whole number of cell parts
n	the number of cell parts
n	the order of Bessel function
$q(x,t)$	body force
r	radius of the solid rod
$r(x)$	non-uniform radius of the solid rod
s	dimensionless distance (coordinate)
t	time
$u(x,t)$	local displacement

$\hat{u}(x)$	amplitude of local displacement
v	wave velocity
w	M_{11} element of transfer matrix
x	distance (coordinate)
z	M_{12} element of transfer matrix

Greek capital letters

Ψ_{R}, Ψ_{L}	wave functions

Greek lowercase letters

α_1 - α_6	expressions (6.51)
β_1 - β_6	expressions (6.56)
$\epsilon_{xx}(x,t)$	extensional strain along x-axis
$\eta(s)$	dimensionless Young's modulus
μ	half of trace of the shifted transfer matrix $\mathbf{P}$
$\xi(s)$	dimensionless mass density
$\rho(x)$	mass density
ρ, ρ_0	constant mass densities
$\sigma(x,t)$	dynamic stress field
$\sigma_{xx}(x,t)$	dynamic stress field along x-axis
ς	infinitesimally small increment
$\phi_{\pm}$	expressions (4.19)
$\varphi_{\pm}$	expressions (4.22)
ω	angular frequency

Roman numerals

I, II, III	solid rod regions

1 Introduction

In isotropic and homogeneous media, there are two kinds of a wave motion: traveling waves, which can have any frequency, and standing waves, which occur only for discrete frequencies. In periodic media, the third kind of motion has been detected, it is characterized by appearance of band gaps separating pass bands (see e.g. [1], [2]). Photonic crystals have presented a such property, that enables nowadays to use them as optical waveguides, high quality resonators, selective filters, lens or super prism (see e.g. [3]). Later it has been discovered that the band gap formation in periodic composite materials also pertains to elastic/acoustic wave propagation. These periodic structures are called phononic crystals, they involve a larger variety of materials as concerns the possibility of high contrast among the elastic properties. Today, phononic crystals have numerous applications such as elastic/acoustic filters, transducer design improvements, noise control, vibration shields, thermal-barrier structures, etc. Furthermore, other interesting properties such as negative refraction or the creation of super lenses have been observed with these structures, which offers other new perspectives for research and application (see e.g. [4]).

The study of crystals and other periodic structures can be precisely described using Bloch's theorem, as long as the infinite number of repetitions is assumed. However, real objects are hardly infinite, they have only a relatively small number N of repeating elements, let us call these systems *locally periodic*, and require another approach (see e.g. [1]). In order to study periodic media with the finite number of repetitions, this work is restricted to a one-dimensional problem in the solid phase. Since the band gap phenomenon occurs for any kind of a wave propagation, such as mechanical, acoustical, electromagnetic and even oceanographic waves, it can be easily applied to any other wave problem (see e.g. [1]). Therefore, the results obtained can be adapted to e.g. sound propagation in a waveguide. The one-dimensional wave propagation problem is presented through the transfer matrix method (see e.g. [1], [2], [5], [6]). The periodic structure can be modelled by a sequence of elementary cells, each of which is described by the transfer matrix. Non-uniform dependencies of mass density and elastic properties are taken into consideration. Since the whole study is done analytically, it imposes strong conditions on the shape of the used cells. The transmission coefficient for the locally periodic structures is calculated with the help of the Chebyshev polynomials. Unlike the previous studies which included only one type of the cell, this work studies different kinds of cells. The goal is to link together the description of the frequency band gaps and the medium's parameters.

The study is organized as follows. Within Chapter 2 the transfer matrix method is presented, the transfer matrix properties are listed, the formula for the transmission coefficient calculation of the locally periodic structures through the Chebyshev polynomials is derived. Chapter 3 is devoted to the modelling the propagation of plane elastic waves in a solid rod. Chapter 4 deals with the two types of the cell: with non-uniform cross-sections, with non-uniform mass densities and Young's moduli. In Chapter 5 the ratio between two parts of the cell on the band gap existence is studied. Chapter 6 is devoted to the elastic wave propagation through the linearly graded material. The positive and negative gradients of Young's modulus is studied and the *triangular* com-

bination of these gradients. The wave of the inhomogeneous region is described by Bessel functions. Chapter 7 states the conclusion.

2 Transfer Matrix

In this chapter a mathematical method for the analysis of a wave propagation in a one-dimensional system is introduced. The method uses the transfer matrix and it is commonly known as the transfer matrix method. The transfer matrix method can be used for the analysis of the elastic waves propagation (see e.g. [2]).

2.1 Scattering Matrix and Transfer Matrix

The first system to be introduced is shown in Fig. 1 in a dimensionless notation and it is called a basic cell. The cell has its characteristics that influences the wave propagation. The wave is divided into the transmitted and the reflected wave at the junctions of the cell. The subscripts L (Left) and R (Right) indicate the position of the wave with respect to the region of the cell, the superscripts + and – determine the direction of the propagation. The wave moves from the left to the right. So, the incoming waves are Ψ_{L}^{+} and Ψ_{R}^{-}, the outgoing waves are Ψ_{L}^{-} and Ψ_{R}^{+} (see e.g. [2]).

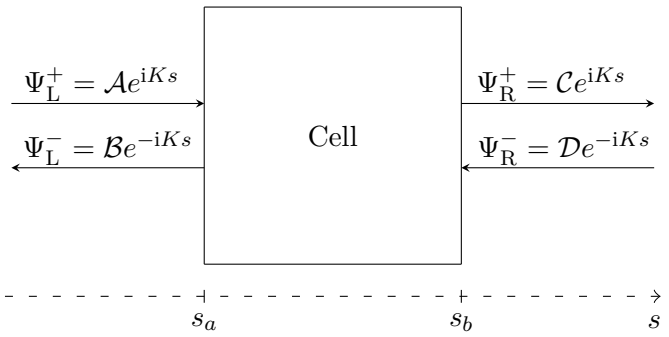

Fig. 1 Transmitted and reflected waves.

The wave functions at the left and right sides of the cell are

$$\Psi_{\mathrm{L}}(s) = \Psi_{\mathrm{L}}^{+}(s) + \Psi_{\mathrm{L}}^{-}(s) = \mathcal{A}e^{\mathrm{i}Ks} + \mathcal{B}e^{-\mathrm{i}Ks} \ , \quad s \leq s_a \ , \tag{2.1}$$

$$\Psi_{\mathrm{R}}(s) = \Psi_{\mathrm{R}}^{+}(s) + \Psi_{\mathrm{R}}^{-}(s) = \mathcal{C}e^{\mathrm{i}Ks} + \mathcal{D}e^{-\mathrm{i}Ks} \ , \quad s \geq s_b \ . \tag{2.2}$$

where $\mathcal{A}$, $\mathcal{B}$, $\mathcal{C}$, $\mathcal{D}$ are complex amplitudes, K is the dimensionless wave number (see e.g. [1], [2], [6]).

In general, linear relations between outgoing and incoming waves can be written as

$$\begin{pmatrix} \Psi_{\mathrm{L}}^{-}(s = s_a) \\ \Psi_{\mathrm{R}}^{+}(s = s_b) \end{pmatrix} = \mathbf{S} \begin{pmatrix} \Psi_{\mathrm{L}}^{+}(s = s_a) \\ \Psi_{\mathrm{R}}^{-}(s = s_b) \end{pmatrix} \ , \tag{2.3}$$

where the scattering matrix $\mathbf{S}$ is

$$\mathbf{S} = \begin{pmatrix} S_{11} & S_{12} \\ S_{21} & S_{22} \end{pmatrix} \ . \tag{2.4}$$

The transfer matrix $\mathbf{P}$ is defined by the following relation

$$\begin{pmatrix} \Psi_{\mathrm{R}}^{+}(s=s_b) \\ \Psi_{\mathrm{R}}^{-}(s=s_b) \end{pmatrix} = \mathbf{P} \begin{pmatrix} \Psi_{\mathrm{L}}^{+}(s=s_a) \\ \Psi_{\mathrm{L}}^{-}(s=s_a) \end{pmatrix} , \tag{2.5}$$

The matrix $\mathbf{P}$ represents a linear correspondence between wave functions on the right-hand side of the cell and the wave functions on the left-hand side (see e.g. [2]).

By substituting the expressions (2.1) and (2.2) with amplitudes and the wave number instead of wave functions, the transfer matrix $\mathbf{P}$ can be written in the way (see e.g. [5])

$$\begin{pmatrix} \mathcal{C}e^{\mathrm{i}Ks_b} \\ \mathcal{D}e^{\mathrm{i}Ks_b} \end{pmatrix} = \mathbf{P} \begin{pmatrix} \mathcal{A}e^{\mathrm{i}Ks_a} \\ \mathcal{B}e^{\mathrm{i}Ks_a} \end{pmatrix} . \tag{2.6}$$

There is also one more definition of the transfer matrix using the linear relationship just between amplitudes $\mathcal{A}$, $\mathcal{B}$, $\mathcal{C}$, $\mathcal{D}$ defined in Eqs. (2.1) and (2.2) (see e.g. [1], [2], [6], [5])

$$\begin{pmatrix} \mathcal{C} \\ \mathcal{D} \end{pmatrix} = \mathbf{M} \begin{pmatrix} \mathcal{A} \\ \mathcal{B} \end{pmatrix} , \tag{2.7}$$

where the transfer matrix $\mathbf{M}$ has the form

$$\mathbf{M} = \begin{pmatrix} M_{11} & M_{12} \\ M_{21} & M_{22} \end{pmatrix} . \tag{2.8}$$

The relation between transfer matrices $\mathbf{P}$ and $\mathbf{M}$ in accordance with the notations in Fig. 1 and after some mathematical manipulations is (see e.g. [1], [2])

$$\mathbf{P} = \begin{pmatrix} e^{\mathrm{i}K(s_b-s_a)} & 0 \\ 0 & e^{-\mathrm{i}K(s_b-s_a)} \end{pmatrix} \mathbf{M} . \tag{2.9}$$

In order to be precise let us call the matrix $\mathbf{M}$ as the transfer matrix, the matrix $\mathbf{P}$ as the *shifted* transfer matrix.

In order to distinguish the different transfer matrices, the *shifted* transfer matrices as well, let us denote the matrices $\mathbf{M}$ and $\mathbf{P}$ with the coordinates denoting the left and right sides of an area described by the transfer matrix. Then the matrices from relation (2.9) can be denoted as $\mathbf{M}(s_b, s_a)$ and $\mathbf{P}(s_b, s_a)$ (see e.g. [5]).

The transfer matrix approach is more appropriate for the analysis of one-dimensional systems than the scattering one. Since the object of study in this master thesis are one-dimensional systems, the transfer matrix approach is chosen to work with.

2.2 Properties of Transfer Matrix

The next properties of the transfer matrix represented by matrix (2.8) and the shifted transfer matrix defined by (2.9) of a cell are considered in the work.

2.2.1 Symmetry

The physical systems that are symmetric with respect to an inversion of time possess symmetry which further reduces the number of independent parameters of the scattering and transfer matrices (see e.g. [2]).

Let the wave moves from the right to the left for the cell presented in Fig. 1. Since the complex conjugate wave function[1] means the propagation in the opposite direction, in a time reversal situation the incoming waves are Ψ_{R}^{+*} and Ψ_{L}^{-*}, the outgoing waves are Ψ_{R}^{-*} and Ψ_{L}^{+*} (see e.g. [2]). After expressing the transfer matrix for this propagation and comparing with the transfer matrix defined by (2.8), the reduction of the independent parameters of matrix $\mathbf{M}(s_b, s_a)$ leads to the form (see e.g. [1], [2], [5], [6])

$$\mathbf{M}(s_b, s_a) = \begin{pmatrix} M_{11} & M_{12} \\ M_{12}^* & M_{11}^* \end{pmatrix} . \tag{2.10}$$

The shifted transfer matrix $\mathbf{P}(s_b, s_a)$ consists of two matrices: the transfer matrix $\mathbf{M}(s_b, s_a)$ and the matrix represented by relation (2.9). Let us call this matrix the factor matrix. The factor matrix also satisfies the symmetry property. Let us multiply the matrices of the shifted transfer matrix, where the transfer matrix $\mathbf{M}(s_b, s_a)$ has the form as written in (2.10), the result matrix also satisfies the symmetry property

$$\mathbf{P}(s_b, s_a) = \begin{pmatrix} e^{\mathrm{i}K(s_b - s_a)} M_{11} & e^{\mathrm{i}K(s_b - s_a)} M_{12} \\ e^{-\mathrm{i}K(s_b - s_a)} M_{12}^* & e^{-\mathrm{i}K(s_b - s_a)} M_{11}^* \end{pmatrix} = \begin{pmatrix} P_{11} & P_{12} \\ P_{12}^* & P_{11}^* \end{pmatrix} . \tag{2.11}$$

2.2.2 Unimodularity

The relationship between the elements of matrix $\mathbf{M}(s_b, s_a)$ is the following (see e.g. [1], [2])

$$|M_{11}|^2 - |M_{12}|^2 = 1 . \tag{2.12}$$

Combining the result above and taking into consideration the form (2.10) of matrix $\mathbf{M}(s_b, s_a)$, the determinant of the transfer matrix is (see e.g. [1], [2])

$$\det \mathbf{M}(s_b, s_a) = M_{11} M_{11}^* - M_{12}^* M_{12} = |M_{11}|^2 - |M_{12}|^2 = 1 , \tag{2.13}$$

which means that the transfer matrix $\mathbf{M}(s_b, s_a)$ is unimodular with the determinant being equal to 1.

The determinant of the factor matrix of the shifted transfer matrix $\mathbf{P}(s_b, s_a)$ is also equal to 1, so the factor matrix is also unimodular. The determinant of a multiplication of two matrices is equal to the multiplication of the determinants, it follows that the shifted transfer matrix is also unimodular.

The determinant of matrices $\mathbf{M}(s_b, s_a)$ and $\mathbf{P}(s_b, s_a)$ can be different from one for some cases, so it is necessary to pay attention for an each type of the cell.

2.2.3 Transmission Coefficient

Let us show how to calculate the transmission coefficient of the cell through the transfer matrix formalism. From Eqs. (2.7) and (2.8) amplitudes $\mathcal{C}$ and $\mathcal{D}$ are equal to

$$\mathcal{C} = M_{11}\mathcal{A} + M_{12}\mathcal{B} , \tag{2.14}$$

$$\mathcal{D} = M_{21}\mathcal{A} + M_{22}\mathcal{B} . \tag{2.15}$$

[1] The complex conjugated variables are marked with an asterisk.

By supposing $\mathcal{D}$ is zero, $\mathcal{B}$ can be expressed from Eq. (2.15) and substituted into Eq. (2.14). Then $\mathcal{C}$ from Eq. (2.14) equals

$$\mathcal{C} = \mathcal{A}\frac{M_{11}M_{22} - M_{12}M_{21}}{M_{22}} , \tag{2.16}$$

where the numerator is the determinant of the transfer matrix.

The transmission coefficient is defined by the ratio of transmitted and incident wave amplitudes, then from Eq. (2.16) an expression for the transmission coefficient is

$$\mathcal{T} = \frac{\mathcal{C}}{\mathcal{A}} = \frac{\det(\mathbf{M}(s_b, s_a))}{M_{22}} . \tag{2.17}$$

Since the amplitudes are generally complex numbers, it is usually sufficient to calculate the modulus of the transmission coefficient

$$|\mathcal{T}| = \left|\frac{\det(\mathbf{M}(s_b, s_a))}{M_{22}}\right| = \frac{1}{|M_{22}|} , \tag{2.18}$$

where relation (2.13) was used.

For the shifted transfer matrix Eq. (2.18) takes the form

$$|\mathcal{T}| = \left|\frac{\det(\mathbf{P}(s_b, s_a))}{P_{22}}\right| = \frac{1}{|P_{22}|} = \frac{1}{|e^{-\mathrm{i}K(s_1-s_0)}M_{22}|} = \frac{1}{|e^{-\mathrm{i}K(s_1-s_0)}|\,|M_{22}|} = \frac{1}{|M_{22}|} . \tag{2.19}$$

So, the transmission coefficient $\mathcal{T}$ is the same for both formulations since the transfer matrices $\mathbf{M}(s_b, s_a)$ and $\mathbf{P}(s_b, s_a)$ differ from each other only in the phase (see e.g. [2]).

2.2.4 Multiplication

If the wave propagates through two cells, then the multiplication property is applied. The first cell to be passed is characterized by $\mathbf{M}(s_b, s_a)$ transfer matrix, the second one by $\mathbf{M}(s_c, s_b)$, then the composition law to get the transfer matrix of the system is (see e.g. [2])

$$\mathbf{M}(s_c, s_a) = \mathbf{M}(s_c, s_b)\mathbf{M}(s_b, s_a) . \tag{2.20}$$

An analogical rule is applied for the shifted transfer matrix

$$\mathbf{P}(s_c, s_a) = \mathbf{P}(s_c, s_b)\mathbf{P}(s_b, s_a) . \tag{2.21}$$

2.3 Transfer Matrix of *N* Cells

Now let us suppose that the basic unit cell introduced in Fig. 1 is replicated N times at regular intervals as in Fig. 2. The goal is to construct the transfer matrix for the whole depicted array based on the given transfer matrix for a single cell (see e.g. [1]).

The length of the basic cell is represented by s_1, the distance between the corresponding sides of the neighboring cells is s_2, the distance between the closest sides of the neighboring cells is l (see e.g. [1]).

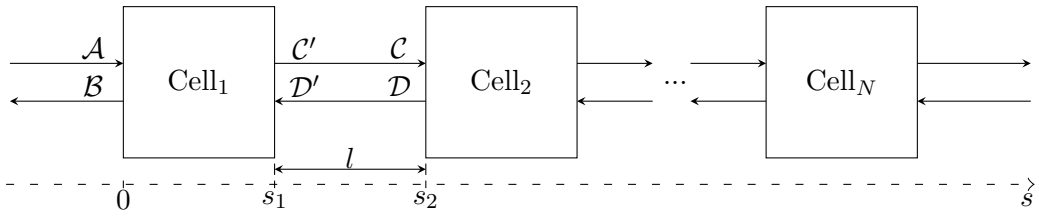

Fig. 2 Finite periodic system in amplitudes notation.

2.3.1 Transfer Matrix of Single Cell

A single cell is represented not only by the basic cell Cell$_1$, but also by the part between coordinates s_1 and s_2, so it is necessary to get the expression relating amplitudes $\mathcal{C}$, $\mathcal{D}$ and $\mathcal{A}$, $\mathcal{B}$ for a chosen type of the cell.

Based on the symmetry and unimodularity properties, let us set up the transfer matrix of Cell$_1$ in the form (see e.g. [1])

$$\mathbf{M}(s_1, 0) = \begin{pmatrix} w & z \\ z^* & w^* \end{pmatrix} , \tag{2.22}$$

where w and z satisfy (see e.g. [1], [2])

$$|w|^2 - |z|^2 = 1 . \tag{2.23}$$

The shifted transfer matrix of Cell$_1$ using relation (2.6) is

$$\begin{pmatrix} \mathcal{C}' e^{\mathrm{i}Ks_1} \\ \mathcal{D}' e^{-\mathrm{i}Ks_1} \end{pmatrix} = \mathbf{P}(s_1, 0) \begin{pmatrix} \mathcal{A} \\ \mathcal{B} \end{pmatrix} . \tag{2.24}$$

The left side of Eq. (2.24) can be expressed as a multiplication of matrices, so Eq. (2.24) can be written as

$$\begin{pmatrix} e^{\mathrm{i}Ks_1} & 0 \\ 0 & e^{-\mathrm{i}Ks_1} \end{pmatrix} \begin{pmatrix} \mathcal{C}' \\ \mathcal{D}' \end{pmatrix} = \mathbf{P}(s_1, 0) \begin{pmatrix} \mathcal{A} \\ \mathcal{B} \end{pmatrix} . \tag{2.25}$$

By multiplying the both sides of Eq. (2.25) by the inverse matrix of the factor matrix, the relation between amplitudes $\mathcal{A}$, $\mathcal{B}$, $\mathcal{C}'$, $\mathcal{D}'$ is given as

$$\begin{pmatrix} \mathcal{C}' \\ \mathcal{D}' \end{pmatrix} = \underbrace{\begin{pmatrix} e^{-\mathrm{i}Ks_1} & 0 \\ 0 & e^{\mathrm{i}Ks_1} \end{pmatrix} \mathbf{P}(s_1, 0)}_{\mathbf{M}(s_1, 0)} \begin{pmatrix} \mathcal{A} \\ \mathcal{B} \end{pmatrix} . \tag{2.26}$$

The shifted transfer matrix $\mathbf{P}(s_1, 0)$ from Eq. (2.26) then equals

$$\mathbf{P}(s_1, 0) = \begin{pmatrix} e^{\mathrm{i}Ks_1} & 0 \\ 0 & e^{-\mathrm{i}Ks_1} \end{pmatrix} \mathbf{M}(s_1, 0) . \tag{2.27}$$

The wave functions at positions $s = s_1 + \varsigma = +s_1$ and $s = s_2 - \varsigma = -s_2$, where ς is an infinitesimally small increment[2], also satisfy Eq. (2.6)

$$\begin{pmatrix} \mathcal{C}e^{\mathrm{i}Ks_2} \\ \mathcal{D}e^{-\mathrm{i}Ks_2} \end{pmatrix} = \mathbf{P}(-s_2, +s_1) \begin{pmatrix} \mathcal{C}'e^{\mathrm{i}Ks_1} \\ \mathcal{D}'e^{-\mathrm{i}Ks_1} \end{pmatrix} . \tag{2.28}$$

The both sides of (2.28) can be expressed as a multiplication of matrices, so the equation can be written as

$$\begin{pmatrix} e^{\mathrm{i}Ks_2} & 0 \\ 0 & e^{-\mathrm{i}Ks_2} \end{pmatrix} \begin{pmatrix} \mathcal{C} \\ \mathcal{D} \end{pmatrix} = \mathbf{P}(-s_2, +s_1) \begin{pmatrix} e^{\mathrm{i}Ks_1} & 0 \\ 0 & e^{-\mathrm{i}Ks_1} \end{pmatrix} \begin{pmatrix} \mathcal{C}' \\ \mathcal{D}' \end{pmatrix} . \tag{2.29}$$

The multiplication of the both sides of Eq. (2.29) by the inverse matrix of the factor matrix on the left side brings to

$$\begin{pmatrix} \mathcal{C} \\ \mathcal{D} \end{pmatrix} = \underbrace{\begin{pmatrix} e^{-\mathrm{i}Ks_2} & 0 \\ 0 & e^{\mathrm{i}Ks_2} \end{pmatrix} \mathbf{P}(-s_2, +s_1) \begin{pmatrix} e^{\mathrm{i}Ks_1} & 0 \\ 0 & e^{-\mathrm{i}Ks_1} \end{pmatrix}}_{\mathbf{M}(-s_2, +s_1) = \text{identity matrix}} \begin{pmatrix} \mathcal{C}' \\ \mathcal{D}' \end{pmatrix} . \tag{2.30}$$

$\mathbf{M}(-s_2, +s_1)$ is the identity matrix, because at the end points on the line segment $(-s_2, +s_1)$ the waves save its amplitudes, but the phases are different. From the equivalence of the transfer and the shifted transfer matrices from Eq. (2.30) matrix $\mathbf{P}(-s_2, +s_1)$ can be expressed as (see e.g. [5])

$$\mathbf{P}(-s_2, +s_1) = \begin{pmatrix} e^{\mathrm{i}K(s_2 - s_1)} & 0 \\ 0 & e^{-\mathrm{i}K(s_2 - s_1)} \end{pmatrix} . \tag{2.31}$$

Finally, the relation between amplitudes $\mathcal{C}$, $\mathcal{D}$ and $\mathcal{A}$, $\mathcal{B}$ are (see e.g. [1])

$$\begin{pmatrix} \mathcal{C} \\ \mathcal{D} \end{pmatrix} = \mathbf{P}(-s_2, 0) \begin{pmatrix} \mathcal{A} \\ \mathcal{B} \end{pmatrix} = \mathbf{P}(-s_2, +s_1)\mathbf{P}(s_1, 0) \begin{pmatrix} \mathcal{A} \\ \mathcal{B} \end{pmatrix} . \tag{2.32}$$

By substituting the expressions of the shifted matrices described by (2.31) and (2.27) accordingly, the amplitudes relationship is

$$\begin{pmatrix} \mathcal{C} \\ \mathcal{D} \end{pmatrix} = \underbrace{\begin{pmatrix} e^{\mathrm{i}Ks_2} & 0 \\ 0 & e^{-\mathrm{i}Ks_2} \end{pmatrix} \mathbf{M}(s_1, 0)}_{\mathbf{P}(-s_2, 0)} \begin{pmatrix} \mathcal{A} \\ \mathcal{B} \end{pmatrix} . \tag{2.33}$$

Let us substitute the expression for $\mathbf{M}(s_1, 0)$ into (2.33) and multiply the matrices to see the final formula of the shifted transfer matrix of the single cell (see e.g. [1])

$$\mathbf{P}(-s_2, 0) = \begin{pmatrix} we^{\mathrm{i}Ks_2} & ze^{\mathrm{i}Ks_2} \\ z^*e^{-\mathrm{i}Ks_2} & w^*e^{-\mathrm{i}Ks_2} \end{pmatrix} . \tag{2.34}$$

[2] One-sided limits: $+s_1$ and $-s_2$ are right-hand and left-hand limits respectively.

If the matrices (2.34) and (2.11) are compared, it is obvious that the derived expression of $\mathbf{P}(s_2, 0)$ satisfies the known formula even if the corresponding cell is a little bit in a different form.

2.3.2 Chebyshev Identity

Once the transfer matrix is calculated for one cell, it can be easily extended to calculate analytically the transfer matrix for N identical cells (see e.g. [1], [2]).

Let us demonstrate that using some transfer matrix properties and a chosen *trick* it is possible to obtain compact and universal expressions for the transfer matrix of a finite periodic system.

Basing on the result from the previous section, let us mention once more the shifted matrix

$$\mathbf{P}(-s_2, 0) = \begin{pmatrix} P_{11} & P_{12} \\ P_{12}^* & P_{11}^* \end{pmatrix} = \begin{pmatrix} we^{\mathrm{i}Ks_2} & ze^{\mathrm{i}Ks_2} \\ z^*e^{-\mathrm{i}Ks_2} & w^*e^{-\mathrm{i}Ks_2} \end{pmatrix} . \tag{2.35}$$

Let us use the multiplicative property of the shifted transfer matrices, then it is possible to write the shifted transfer matrix of the sequence of N-cells as (see e.g. [5])

$$\mathbf{P}_N = \underbrace{\mathbf{P}(-[Ns_2], (N-1)s_2).\mathbf{P}(-[(N-1)s_2], (N-2)s_2)...\mathbf{P}(-s_2, 0)}_{N \text{ factors}} = \mathbf{P}^N . \tag{2.36}$$

Eq. (2.36) can be shortly written as

$$\mathbf{P}_N = \underbrace{\mathbf{P}...\mathbf{P}}_{N\text{-1 factors}} .\mathbf{P} = \mathbf{P}_{N-1}.\mathbf{P}(-s_2, 0) . \tag{2.37}$$

Eq. (2.37) means that the product of matrices can be written as the product of the last $N-1$ matrices denoted as $\mathbf{P}_{N-1}$ and the first matrix $\mathbf{P}(-s_2, 0)$. So, having the transfer matrix of the single cell only is sufficient to get the shifted transfer matrix of the sequence of N-cells (see e.g. [5]).

In the terms of matrices, the expression above can be rewritten as

$$\mathbf{P}_N = \begin{pmatrix} P_{N_{11}} & P_{N_{12}} \\ P_{N_{12}}^* & P_{N_{11}}^* \end{pmatrix} = \begin{pmatrix} P_{(N-1)_{11}} & P_{(N-1)_{12}} \\ P_{(N-1)_{12}}^* & P_{(N-1)_{11}}^* \end{pmatrix} \begin{pmatrix} P_{11} & P_{12} \\ P_{12}^* & P_{11}^* \end{pmatrix} . \tag{2.38}$$

Now, let us obtain $P_{N_{11}}$ and $P_{N_{12}}$ through the known P_{11} and P_{12}. From Eq. (2.38)

$$P_{N_{11}} = P_{(N-1)_{11}} P_{11} + P_{(N-1)_{12}} P_{12}^* , \tag{2.39}$$

$$P_{N_{12}} = P_{(N-1)_{11}} P_{12} + P_{(N-1)_{12}} P_{11}^* . \tag{2.40}$$

Let us express $P_{(N-1)_{11}}$ from Eq. (2.40)

$$P_{(N-1)_{11}} = P_{N_{12}} P_{12}^{-1} - P_{(N-1)_{12}} P_{11}^* P_{12}^{-1} . \tag{2.41}$$

Let us define the function

$$p_{N-1} = P_{N_{12}} P_{12}^{-1} \rightarrow P_{N_{12}} = P_{12} p_{N-1} , \tag{2.42}$$

then Eq. (2.41) can be rewritten as

$$P_{(N-1)_{11}} = p_{N-1} - p_{N-2} P_{11}^* \quad \text{or} \quad P_{N_{11}} = p_N - p_{N-1} P_{11}^* . \tag{2.43}$$

By substituting Eq. (2.42) and Eq. (2.43) into Eq. (2.39), the following recurrence relation is obtained

$$p_N - (P_{11} + P_{11}^*)\, p_{N-1} + p_{N-2} = 0\ . \tag{2.44}$$

To solve this equation it is necessary to define the initial conditions. Let us consider that:

1. $\mathbf{P}_0 = \mathbf{I} \rightarrow P_{0_{11}} = P_{0_{11}}^* = 1,\ P_{0_{12}} = P_{0_{12}}^* = 0,$
2. $\mathbf{P}_1 = \mathbf{P} \rightarrow P_{1_{11}} = P_{11},\ P_{1_{11}}^* = P_{11}^*,\ P_{1_{12}} = P_{12},\ P_{1_{12}}^* = P_{12}^*,$
3. from Eq. (2.42) and 2. follows $p_0 = 1,$
4. from Eq. (2.42) and 1. follows $p_{-1} = 0,$
5. the trace is

$$\mu = \frac{1}{2}\mathrm{Tr}(\mathbf{P}(-s_2, 0)) = \frac{1}{2}\left(P_{11} + P_{11}^*\right) = \frac{1}{2}\left(we^{\mathrm{i}Ks_2} + w^* e^{-\mathrm{i}Ks_2}\right)\ . \tag{2.45}$$

The recurrence Eq. (2.44) then is exactly the same as Eq. (2.46).

Equation

$$U_N(x) - 2xU_{N-1}(x) + U_{N-2}(x) = 0 \tag{2.46}$$

defines the Chebyshev polynomials of the second kind $U_N(x)$ with $U_0 = 1$ and $U_{-1} = 0$. Therefore, the functions p_N in Eq. (2.44) are the Chebyshev polynomials evaluated at μ (see e.g. [1], [5]). So, let us use notation $U_N(\mu)$ further in this work.

2.3.3 Transfer Matrix of *N* cells

Using relations (2.43), the shifted transfer matrix for N cells has the form

$$\mathbf{P}_N = \begin{pmatrix} U_N(\mu) - P_{11}^* U_{N-1}(\mu) & P_{12}U_{N-1}(\mu) \\ P_{12}^* U_{N-1}(\mu) & U_N(\mu) - P_{11}U_{N-1}(\mu) \end{pmatrix}\ . \tag{2.47}$$

From Eq. (2.33) it is known that

$$\mathbf{P}(-s_2, 0) = \begin{pmatrix} e^{\mathrm{i}Ks_2} & 0 \\ 0 & e^{-\mathrm{i}Ks_2} \end{pmatrix} \mathbf{M}(s_1, 0)\ . \tag{2.48}$$

Based on the results about $\mathbf{P}_N$ from the subsection Chebyshev Identity, using relation (2.48) between the shifted transfer and transfer matrices of the single cell and substituting the expressions of the shifted transfer matrix elements from (2.35), it follows that the transfer matrix for the whole array of N cells is (see e.g. [1])

$$\begin{aligned} \mathbf{M}_N &= \begin{pmatrix} e^{-\mathrm{i}KNs_2} & 0 \\ 0 & e^{\mathrm{i}KNs_2} \end{pmatrix} \mathbf{P}_N \\ &= \begin{pmatrix} e^{-\mathrm{i}KNs_2}\left[U_N(\mu) - w^* e^{-\mathrm{i}Ks_2} U_{N-1}(\mu)\right] & ze^{-\mathrm{i}K(N-1)s_2} U_{N-1}(\mu) \\ z^* e^{\mathrm{i}K(N-1)s_2} U_{N-1}(\mu) & e^{\mathrm{i}KNs_2}\left[U_N(\mu) - we^{\mathrm{i}Ks_2} U_{N-1}(\mu)\right] \end{pmatrix}. \end{aligned} \tag{2.49}$$

From expression (2.49) it is possible to see that to determine the transfer matrix of the periodic system consisting of N cells, it is sufficient only to know the transfer matrix of one cell, i.e. if z and w are known (see e.g. [1]).

Based on the expression of the transmission coefficient (2.19) and using the unimodularity property (2.12), the transmission coefficient modulus in a second power can be found as (see e.g. [1])

$$|\mathcal{T}|^2 = \frac{1}{|M_{22}|^2} = \frac{1}{1 + |M_{12}|^2} \,, \tag{2.50}$$

this last expression is better to apply since it uses less calculations that reduces the calculation error.

Thus, the transmission coefficient modulus of the system of N cells shown in Fig. 2 with using the relation of $M_{N_{12}}$ from (2.49) can be determined by (see e.g. [1])

$$|\mathcal{T}_N| = \frac{1}{\sqrt{1 + [|z|\, U_{N-1}(\mu)]^2}} \,. \tag{2.51}$$

3 Propagation of Elastic Waves in Solid Rod

In this chapter the equation modelling the propagation of plane elastic waves in a solid rod is derived. The solid rod is symmetric along the x-axis, as shown in Fig. 3, with the non-uniform values of cross-section $A(x)$, mass density $\rho(x)$ and Young's modulus $E(x)$. The dynamic stress field $\sigma(x,t)$ causing the local displacement $u(x,t)$, where t is the time, has place. The body force $q(x,t)$ is not considered.

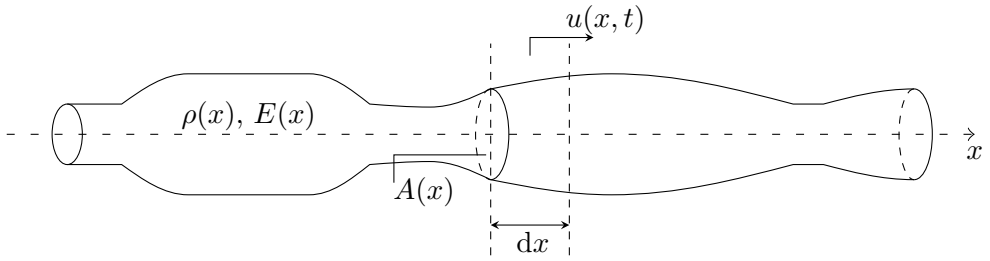

Fig. 3 Non-uniform axially symmetric solid rod.

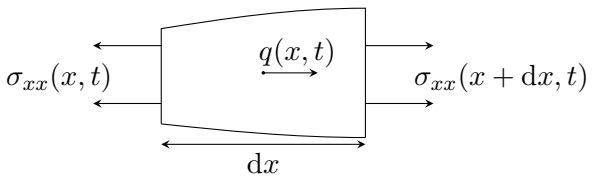

Fig. 4 Differential element of the solid rod under stress $\sigma_{xx}(x,t)$ and with body force $q(x,t)$.

Let us reference an example of a small part of the solid rod as shown in Fig 4, Newton's second law of motion can be written as (see e.g. [7])

$$\rho(x)A(x)\frac{\partial^2 u(x,t)}{\partial t^2}\mathrm{d}x = \sigma_{xx}(x+\mathrm{d}x,t)A(x+\mathrm{d}x) - \sigma_{xx}(x,t)A(x)\ . \tag{3.1}$$

In a pure longitudinal wave motion the direction of a particle displacement is purely in the direction of the wave propagation (see e.g. [7]), then Hooke's law can be written as

$$\sigma_{xx}(x,t) = E(x)\epsilon_{xx}(x,t)\ , \tag{3.2}$$

where $\epsilon_{xx}(x,t)$ is the extensional strain, $\sigma_{xx}(x,t)$ and $\epsilon_{xx}(x,t)$ are the scalar functions. The relation of the extensional strain and the local displacement is

$$\epsilon_{xx}(x,t) = \frac{\partial u(x,t)}{\partial x}\ . \tag{3.3}$$

Using this fact, Eq. (3.1) can be rewritten as

$$\rho(x)A(x)\frac{\partial^2 u(x,t)}{\partial t^2}\mathrm{d}x = E(x+\mathrm{d}x)A(x+\mathrm{d}x)\frac{\partial u(x+\mathrm{d}x,t)}{\partial x} - E(x)A(x)\frac{\partial u(x,t)}{\partial x} \ . \quad (3.4)$$

Let us consider the small elastic wave amplitudes, so only the first order approximation of the dependent variables is taken into account

$$\begin{aligned} u(x+\mathrm{d}x,t) &\approx u(x,t) + \frac{\partial u(x,t)}{\partial x}\mathrm{d}x \ , \\ A(x+\mathrm{d}x) &\approx A(x) + \frac{\mathrm{d}A(x)}{\mathrm{d}x}\mathrm{d}x \ , \\ E(x+\mathrm{d}x) &\approx E(x) + \frac{\mathrm{d}E(x)}{\mathrm{d}x}\mathrm{d}x \ , \\ \rho(x+\mathrm{d}x) &\approx \rho(x) + \frac{\mathrm{d}\rho(x)}{\mathrm{d}x}\mathrm{d}x \ . \end{aligned} \quad (3.5)$$

By substituting the appropriate expressions from the above approximations into Eq. (3.4)

$$\begin{aligned} &\rho(x)A(x)\frac{\partial^2 u(x,t)}{\partial t^2}\mathrm{d}x \\ &= \left[E(x) + \frac{\mathrm{d}E(x)}{\mathrm{d}x}\mathrm{d}x\right]\left[A(x) + \frac{\mathrm{d}A(x)}{\mathrm{d}x}\mathrm{d}x\right]\frac{\partial}{\partial x}\left[u(x,t) + \frac{\partial u(x,t)}{\partial x}\mathrm{d}x\right] - E(x)A(x)\frac{\partial u(x,t)}{\partial x} \\ &= E(x)A(x)\frac{\partial^2 u(x,t)}{\partial x^2}\mathrm{d}x + E(x)\frac{\mathrm{d}A(x)}{\mathrm{d}x}\frac{\partial u(x,t)}{\partial x}\mathrm{d}x + E(x)\frac{\mathrm{d}A(x)}{\mathrm{d}x}\frac{\partial^2 u(x,t)}{\partial x^2}\mathrm{d}x^2 \\ &\quad + \frac{\mathrm{d}E(x)}{\mathrm{d}x}A(x)\frac{\partial u(x,t)}{\partial x}\mathrm{d}x + \frac{\mathrm{d}E(x)}{\mathrm{d}x}A(x)\frac{\partial^2 u(x,t)}{\partial x^2}\mathrm{d}x^2 \\ &\quad + \frac{\mathrm{d}E(x)}{\mathrm{d}x}\frac{\mathrm{d}A(x)}{\mathrm{d}x}\mathrm{d}x^2\left[\frac{\partial u(x,t)}{\partial x} + \frac{\partial^2 u(x,t)}{\partial x^2}\mathrm{d}x\right] \ . \end{aligned} \quad (3.6)$$

After neglecting the second order and the higher terms and reducing $\mathrm{d}x$

$$\rho(x)A(x)\frac{\partial^2 u(x,t)}{\partial t^2} = E(x)A(x)\frac{\partial^2 u(x,t)}{\partial x^2} + E(x)\frac{\mathrm{d}A(x)}{\mathrm{d}x}\frac{\partial u(x,t)}{\partial x} + \frac{\mathrm{d}E(x)}{\mathrm{d}x}A(x)\frac{\partial u(x,t)}{\partial x} \ . \quad (3.7)$$

Can be noticed, that Eq. (3.7) can be rewritten into

$$\rho(x)A(x)\frac{\partial^2 u(x,t)}{\partial t^2} = \frac{\partial}{\partial x}\left[E(x)A(x)\frac{\partial u(x,t)}{\partial x}\right] \ . \quad (3.8)$$

Assuming a time periodic motion

$$u(x,t) = \hat{u}(x)e^{-\mathrm{i}\omega t} \ , \quad (3.9)$$

where ω is the angular frequency and i is the imaginary unit, and substituting this expression of the local displacement into Eq. (3.8), the equation can be written as

$$-\rho(x)A(x)\omega^2\hat{u}(x) = \frac{\mathrm{d}}{\mathrm{d}x}\left[E(x)A(x)\frac{\mathrm{d}\hat{u}(x)}{\mathrm{d}x}\right] \ . \quad (3.10)$$

Equation (3.10) can be expressed as

$$\frac{\mathrm{d}^2\hat{u}(x)}{\mathrm{d}x^2} + \frac{1}{E(x)}\frac{\mathrm{d}E(x)}{\mathrm{d}x}\frac{\mathrm{d}\hat{u}(x)}{\mathrm{d}x} + \frac{1}{A(x)}\frac{\mathrm{d}A(x)}{\mathrm{d}x}\frac{\mathrm{d}\hat{u}(x)}{\mathrm{d}x} + \frac{\rho(x)}{E(x)}\omega^2\hat{u}(x) = 0 \ . \quad (3.11)$$

For solving model equation (3.11), it is convenient to rewrite it into the dimensionless form

$$\frac{\mathrm{d}^2\hat{U}(s)}{\mathrm{d}s^2} + \frac{1}{\eta(s)}\frac{\mathrm{d}\eta(s)}{\mathrm{d}s}\frac{\mathrm{d}\hat{U}(s)}{\mathrm{d}s} + \frac{1}{S(s)}\frac{\mathrm{d}S(s)}{\mathrm{d}s}\frac{\mathrm{d}\hat{U}(s)}{\mathrm{d}s} + \frac{\xi(s)}{\eta(s)}K^2\hat{U}(s) = 0\ . \tag{3.12}$$

Here

$$\begin{aligned} s &= \frac{x}{\ell}\ , \qquad \hat{U}(s) = \frac{\hat{u}(s)}{\ell}\ , \qquad S(s) = \frac{A(s)}{\ell^2}\ , \qquad \eta(s) = \frac{E(s)}{E_0}\ , \\ \xi(s) &= \frac{\rho(s)}{\rho_0}\ , \qquad K^2 = \frac{\omega^2\ell^2}{c_{L0}^2}\ , \qquad c_{L0} = \sqrt{\frac{E_0}{\rho_0}}\ , \end{aligned} \tag{3.13}$$

where ℓ is a characteristic length.

Assuming $E(s) = E_0$ and $\rho(s) = \rho_0$ to be constant, Eq. (3.12) can be reduced to the Webster equation (see e.g. [8], [9])

$$\frac{\mathrm{d}^2\hat{U}(s)}{\mathrm{d}s^2} + \frac{1}{S(s)}\frac{\mathrm{d}S(s)}{\mathrm{d}s}\frac{\mathrm{d}\hat{U}(s)}{\mathrm{d}s} + K^2\hat{U}(s) = 0\ . \tag{3.14}$$

Since $S(s) = \pi r^2(s)/\ell^2$, Eq. (3.14) can be rewritten as

$$\frac{\mathrm{d}^2\hat{U}(s)}{\mathrm{d}s^2} + \frac{2}{R(s)}\frac{\mathrm{d}R(s)}{\mathrm{d}s}\frac{\mathrm{d}\hat{U}(s)}{\mathrm{d}s} + K^2\hat{U}(s) = 0\ , \tag{3.15}$$

where $R(s) = r(s)/\ell$ is the dimensionless radius of the solid rod.

4 Elastic Wave Propagation

In this chapter the general method for the calculation of the transmission coefficient of a wave propagating through an area of a varying cross-section or different materials is presented.

4.1 Single Cell

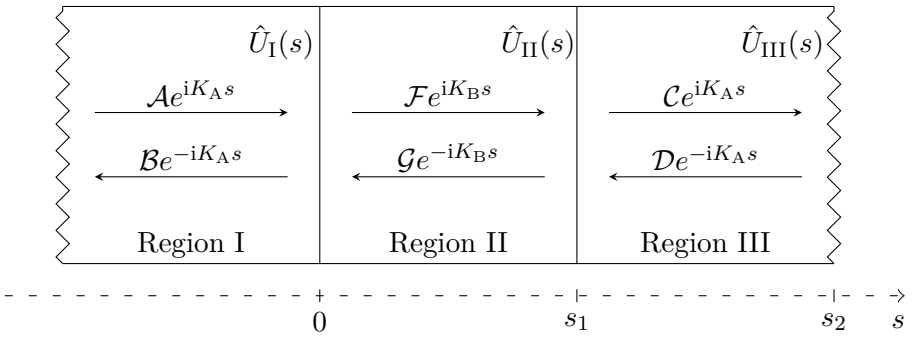

Fig. 5 Reflection and transmission of the wave in a single cell.

Let us assume a solid rod consisting of cells. One cell of the solid rod starts at $s = 0$ and ends at $s = s_2$, so it includes two regions: Region II and Region III. A such unit cell is sketched in Fig. 5. Here the wave propagates from the left to the right, the dimensionless notations for the local displacements in the corresponding regions are marked and they can be expressed as

$$\hat{U}_{\mathrm{I}}(s) = \mathcal{A}e^{\mathrm{i}K_{\mathrm{A}}s} + \mathcal{B}e^{-\mathrm{i}K_{\mathrm{A}}s} \,, \tag{4.1}$$

$$\hat{U}_{\mathrm{II}}(s) = \mathcal{F}e^{\mathrm{i}K_{\mathrm{B}}s} + \mathcal{G}e^{-\mathrm{i}K_{\mathrm{B}}s} \,, \tag{4.2}$$

$$\hat{U}_{\mathrm{III}}(s) = \mathcal{C}e^{\mathrm{i}K_{\mathrm{A}}s} + \mathcal{D}e^{-\mathrm{i}K_{\mathrm{A}}s} \,. \tag{4.3}$$

Roman numerals are used in general description, notations A and B correspond to the defined regions. So, the subscripts A and B are used for the regions with *smaller* and *bigger* cross-section respectively. For the cell with different materials alternating notation corresponds to the type of material.

To find the boundary conditions at the junctions of regions in order to find the elements of the transfer matrix it is necessary to take into account the balance of forces and the continuity of velocities at the junctions $s = 0$ and $s = s_1$ (see e.g. [1])

$$\begin{aligned} F_1 &= F_2 \,, \\ v_1 &= v_2 \,, \end{aligned} \tag{4.4}$$

where indices 1 and 2 mean two regions to the common junction.

4.1.1 Non-Uniform Cross-Section

Let us consider a unit cell with its preceding region as sketched in Fig. 6. The unit cell itself starts at $s = 0$ and ends at $s = s_2$. Here, the cross-sections in regions I and III are equal. The material is the same in all neighboring regions, so the wave numbers K_A and K_B can be identified as K.

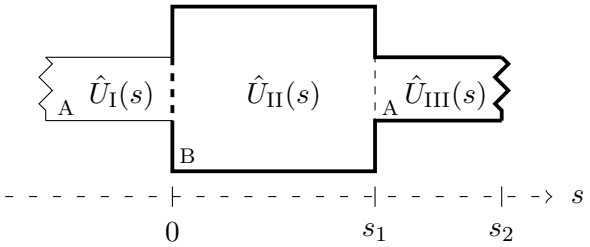

Fig. 6 A unit cell for a non-uniform cross-section.

Let us rewrite the boundary conditions (4.4) for this case. It is helpful to write

$$\begin{aligned} F &= A\sigma_{xx} = AE\epsilon_{xx} = AE\frac{\partial u(x,t)}{\partial x} \,, \\ v &= \frac{\partial u(x,t)}{\partial t} \,. \end{aligned} \tag{4.5}$$

Applying expressions (4.4) and (4.5), the next equalities are applied at junctions $s = 0$ and $s = s_1$

$$\begin{aligned} A_1\frac{\partial u_1(x,t)}{\partial x} &= A_2\frac{\partial u_2(x,t)}{\partial x} \,, \\ \frac{\partial u_1(x,t)}{\partial t} &= \frac{\partial u_2(x,t)}{\partial t} \,. \end{aligned} \tag{4.6}$$

By substituting Eq. (3.9), using relations $s = x/\ell$ and $\hat{U}(s) = \hat{u}(s)/\ell$ and making the reduces, Eqs. (4.6) can be written as

$$\begin{aligned} \frac{A_1(s)}{A_2(s)}\frac{\mathrm{d}\hat{U}_1(s)}{\mathrm{d}s} &= \frac{\mathrm{d}\hat{U}_2(s)}{\mathrm{d}s} \,, \\ \hat{U}_1(s) &= \hat{U}_2(s) \end{aligned} \tag{4.7}$$

The boundary conditions (see e.g. [1]) at the points $s = 0$ and $s = s_1$ then could be written as

$$\begin{aligned} \hat{U}_\mathrm{I}\Big|_{s=-0} &= \hat{U}_\mathrm{II}\Big|_{s=+0} \,, \\ A_\mathrm{A}\frac{\mathrm{d}\hat{U}_\mathrm{I}}{\mathrm{d}s}\bigg|_{s=-0} &= A_\mathrm{B}\frac{\mathrm{d}\hat{U}_\mathrm{II}}{\mathrm{d}s}\bigg|_{s=+0} \,, \\ \hat{U}_\mathrm{III}\Big|_{s=+s_1} &= \hat{U}_\mathrm{II}\Big|_{s=-s_1} \,, \\ A_\mathrm{A}\frac{\mathrm{d}\hat{U}_\mathrm{III}}{\mathrm{d}s}\bigg|_{s=+s_1} &= A_\mathrm{B}\frac{\mathrm{d}\hat{U}_\mathrm{II}}{\mathrm{d}s}\bigg|_{s=-s_1} \,. \end{aligned} \tag{4.8}$$

Applying Eqs. (4.1) - (4.3), it is possible to get the final relationships to work with

$$\begin{aligned} \mathcal{A} + \mathcal{B} &= \mathcal{F} + \mathcal{G} \,, \\ A_\mathrm{A}\left(\mathcal{A} - \mathcal{B}\right) &= A_\mathrm{B}\left(\mathcal{F} - \mathcal{G}\right) \,, \\ \mathcal{C}e^{\mathrm{i}Ks_1} + \mathcal{D}e^{-\mathrm{i}Ks_1} &= \mathcal{F}e^{\mathrm{i}Ks_1} + \mathcal{G}e^{-\mathrm{i}Ks_1} \,, \\ A_\mathrm{A}\left(\mathcal{C}e^{\mathrm{i}Ks_1} - \mathcal{D}e^{-\mathrm{i}Ks_1}\right) &= A_\mathrm{B}\left(\mathcal{F}e^{\mathrm{i}Ks_1} - \mathcal{G}e^{-\mathrm{i}Ks_1}\right) \,. \end{aligned} \tag{4.9}$$

4.1.2 Non-Uniform Mass Density and Young's Modulus

Let us consider a unit cell with its preceding region as sketched in Fig. 7. The unit cell itself starts at $s = 0$ and ends at $s = s_2$. Here, the mass densities and Young's modulus in regions I and III are equal, the cross-sections are the same in all regions.

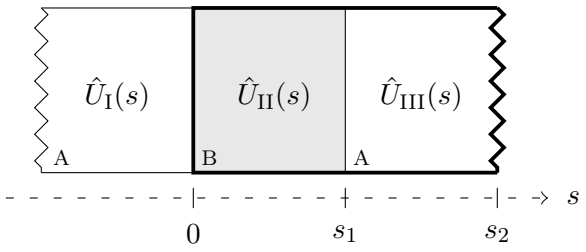

Fig. 7 A unit cell for a non-uniform mass density and Young's modulus.

Let us repeat the boundary conditions (4.4) once more, so as in the previous case

$$\begin{aligned} F = A\sigma_{xx} = AE\epsilon_{xx} = AE\frac{\partial u(x,t)}{\partial x} \,, \\ v = \frac{\partial u(x,t)}{\partial t} \,. \end{aligned} \tag{4.10}$$

So, taking into account expressions (4.4) and (4.10), the next equalities are applied at the junctions $s = 0$ and $s = s_1$

$$\begin{aligned} E_1\frac{\partial u_1(x,t)}{\partial x} = E_2\frac{\partial u_2(x,t)}{\partial x} \,, \\ \frac{\partial u_1(x,t)}{\partial t} = \frac{\partial u_2(x,t)}{\partial t} \,. \end{aligned} \tag{4.11}$$

The dimensionless notation of the boundary conditions above, using (3.9) and relations $s = x/\ell$ and $\hat{U}(s) = \hat{u}(s)/\ell$ as in the previous case, can be written as

$$\begin{aligned} \frac{E_1(s)}{E_2(s)}\frac{\mathrm{d}\hat{U}_1(s)}{\mathrm{d}s} = \frac{\mathrm{d}\hat{U}_2(s)}{\mathrm{d}s} \,, \\ \hat{U}_1(s) = \hat{U}_2(s) \,. \end{aligned} \tag{4.12}$$

At points $s = 0$ and $s = s_1$ the relationships between the regions can be expressed as

$$\begin{aligned} \hat{U}_{\mathrm{I}}\Big|_{s=-0} &= \hat{U}_{\mathrm{II}}\Big|_{s=+0} \,, \\ E_{\mathrm{A}}\frac{\mathrm{d}\hat{U}_{\mathrm{I}}}{\mathrm{d}s}\Big|_{s=-0} &= E_{\mathrm{B}}\frac{\mathrm{d}\hat{U}_{\mathrm{II}}}{\mathrm{d}s}\Big|_{s=+0} \,, \\ \hat{U}_{\mathrm{III}}\Big|_{s=+s_1} &= \hat{U}_{\mathrm{II}}\Big|_{s=-s_1} \,, \\ E_{\mathrm{A}}\frac{\mathrm{d}\hat{U}_{\mathrm{III}}}{\mathrm{d}s}\Big|_{s=+s_1} &= E_{\mathrm{B}}\frac{\mathrm{d}\hat{U}_{\mathrm{II}}}{\mathrm{d}s}\Big|_{s=-s_1} \,. \end{aligned} \tag{4.13}$$

Taking into account Eqs. (4.1) - (4.3), it is possible to get the final relationships to work with

$$\begin{aligned} \mathcal{A} + \mathcal{B} &= \mathcal{F} + \mathcal{G} \,, \\ E_{\mathrm{A}}K_{\mathrm{A}}\left(\mathcal{A} - \mathcal{B}\right) &= E_{\mathrm{B}}K_{\mathrm{B}}\left(\mathcal{F} - \mathcal{G}\right) \,, \\ \mathcal{C}e^{\mathrm{i}K_{\mathrm{A}}s_1} + \mathcal{D}e^{-\mathrm{i}K_{\mathrm{A}}s_1} &= \mathcal{F}e^{\mathrm{i}K_{\mathrm{B}}s_1} + \mathcal{G}e^{-\mathrm{i}K_{\mathrm{B}}s_1} \,, \\ E_{\mathrm{A}}K_{\mathrm{A}}\left(\mathcal{C}e^{\mathrm{i}K_{\mathrm{A}}s_1} - \mathcal{D}e^{-\mathrm{i}K_{\mathrm{A}}s_1}\right) &= E_{\mathrm{B}}K_{\mathrm{B}}\left(\mathcal{F}e^{\mathrm{i}K_{\mathrm{B}}s_1} - \mathcal{G}e^{-\mathrm{i}K_{\mathrm{B}}s_1}\right) \,. \end{aligned} \tag{4.14}$$

4.2 Multiple Cells

Replicating N times the unit cell for both investigated cases, the multiple cells solid rods then look like in Fig. 8 and Fig. 12. These arrangements represent one-dimensional phononic crystals.

From subsection 2.3.3 it is known, that to determine the transfer matrix of the periodic system consisting of N cells it is sufficient only to know w and z, which are connected to the transfer matrix of the part of the cell, that is from $s = 0$ to $s = s_1$ (see e.g. [1]). By substituting appropriate wave numbers K_A and K_B instead of K (this distinction is important for the solid rod consisting of different materials), the transfer matrix of N cells then is

$$\mathbf{M}_N = \begin{pmatrix} e^{-\mathrm{i}K_\mathrm{A}Ns_2}\left[U_N(\mu) - w^* e^{-\mathrm{i}K_\mathrm{A}s_2}U_{N-1}(\mu)\right] & ze^{-\mathrm{i}K_\mathrm{A}(N-1)s_2}U_{N-1}(\mu) \\ z^* e^{\mathrm{i}K_\mathrm{A}(N-1)s_2}U_{N-1}(\mu) & e^{\mathrm{i}K_\mathrm{A}Ns_2}\left[U_N(\mu) - we^{\mathrm{i}K_\mathrm{A}s_2}U_{N-1}(\mu)\right] \end{pmatrix} . \tag{4.15}$$

The Chebyshev polynomials are evaluated at μ, where μ is

$$\mu = \frac{1}{2}\left(we^{\mathrm{i}K_\mathrm{A}s_2} + w^* e^{-\mathrm{i}K_\mathrm{A}s_2}\right) . \tag{4.16}$$

The transmission coefficient of N cells then is found with the help of derived expression

$$|\mathcal{T}_N| = \frac{1}{\sqrt{1 + \left[|z|\, U_{N-1}(\mu)\right]^2}} . \tag{4.17}$$

4.2.1 Non-Uniform Cross-Section

The solid rod consisting of N multiple cells, where the single cell consists of the two part with different cross-sections of the same material as was discussed earlier, is represented in Fig. 8.

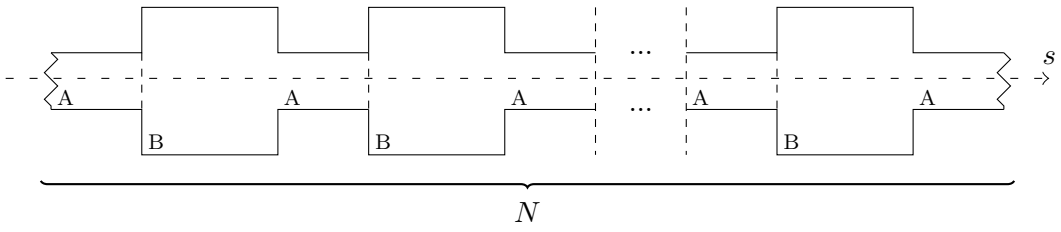

Fig. 8 An array of cells for a non-uniform cross-section.

By identifying the wave numbers in regions since the material is the same, the required elements of the transfer matrix for this case are

$$\begin{aligned} w &= e^{\mathrm{i}Kl}\left[\cos(Ks_1) + \mathrm{i}\phi_+ \sin(Ks_1)\right] , \\ z &= -\mathrm{i}e^{\mathrm{i}Kl}\phi_- \sin(Ks_1) , \\ \mu &= \cos(Kl)\cos(Ks_1) - \phi_+ \sin(Kl)\sin(Ks_1) , \end{aligned} \tag{4.18}$$

where

$$\phi_\pm = \frac{1}{2}\left(\frac{A_\mathrm{A}}{A_\mathrm{B}} \pm \frac{A_\mathrm{B}}{A_\mathrm{A}}\right) , \quad A_\mathrm{A} = \pi r_\mathrm{A}^2 , \quad A_\mathrm{B} = \pi r_\mathrm{B}^2 , \quad K = \frac{2\pi f\ell}{\sqrt{E/\rho}} . \tag{4.19}$$

The transmission coefficient of the N repeating cells can be found through

$$|\mathcal{T}_N| = \frac{1}{\sqrt{1 + \left[|\phi_- \sin(Ks_1)|\, U_{N-1}(\mu)\right]^2}} . \tag{4.20}$$

In the work [1] it is shown that with the increasing values of N the emergence of a large frequency gap has a place. Let us see how it is possible to reduce the amount of the cells by choosing appropriate parameters values of the solid rod and how the parameters of a band gap can be influenced by these values.

The transmitted wave over frequencies is influenced by the ratio of cross-sections radii. The bigger this ratio the less part of the wave is transmitted for some band. The illustration to this conclusion is shown in Fig. 9. These results are for one cell with chosen values of parameters $\ell = 1$ m, $s_1 = 4$ cm, $l = 2$ cm for aluminum characterized by $\rho = 2.7$ g/cm^3 and $E = 69$ GPa. The chosen value of radius r_A is 1 cm, r_B is 2 cm, 5 cm and 10 cm (that values correspond to ratios 2, 5 and 10 respectively). The order of cross-sections for one cell doesn't influence the transmission coefficient for the chosen values.

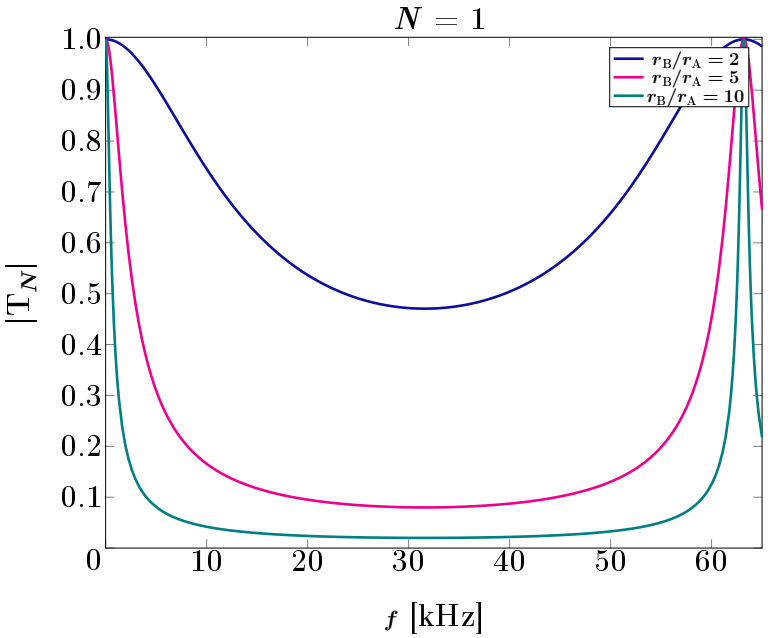

Fig. 9 Dependence of the transmission coefficient modulus on frequency for non-uniform cross-sections for different ratio of radii (aluminum).

The chosen material influences the frequency and the range of the possible band gaps. This conclusion can be seen from Fig. 10, the chosen materials are aluminum (Al), nickel (Ni) with $\rho = 8.88$ g/cm^3 and $E = 199.5$ GPa, silicon carbide (SiC) with $\rho = 3.1$ g/cm^3 and $E = 427$ GPa, steel with $\rho = 7.75$ g/cm^3 and $E = 200$ GPa, the rest parameters values are remained the same.

The emergence of the bang gap can be already got for just $N = 2$ cells. An example of that fact can be seen in Fig. 11. Nickel is chosen with the ratio of radii of 10. The drop before the band gap has place.

By adding more cells the band gap form is adjusted to the right angles. The increase of the cells shifts the band gap to the higher frequencies and decrease the range of frequencies. In Fig. 11 these facts are shown for $N = 24$ cells.

4.2.2 Non-Uniform Mass Density and Young's Modulus

The solid rod consisting of N multiple cells, where the single cell consists of the two parts with different mass densities and Young's moduli as was discussed earlier, is represented in Fig. 12.

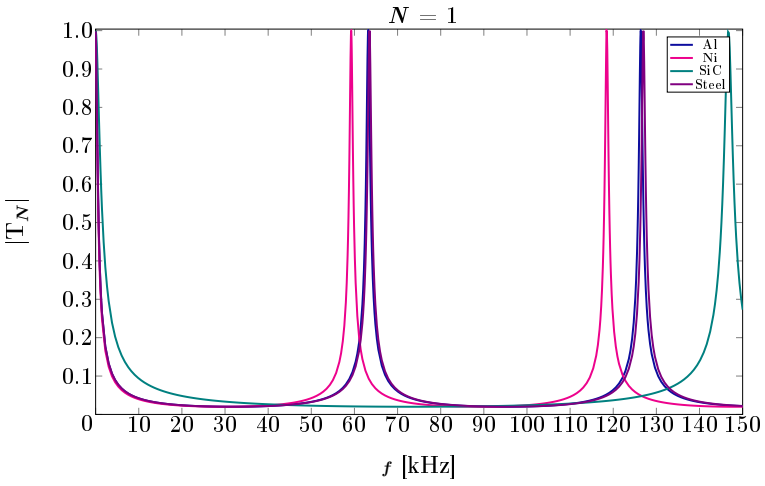

Fig. 10 Dependence of the transmission coefficient modulus on frequency for non-uniform cross-sections from different materials.

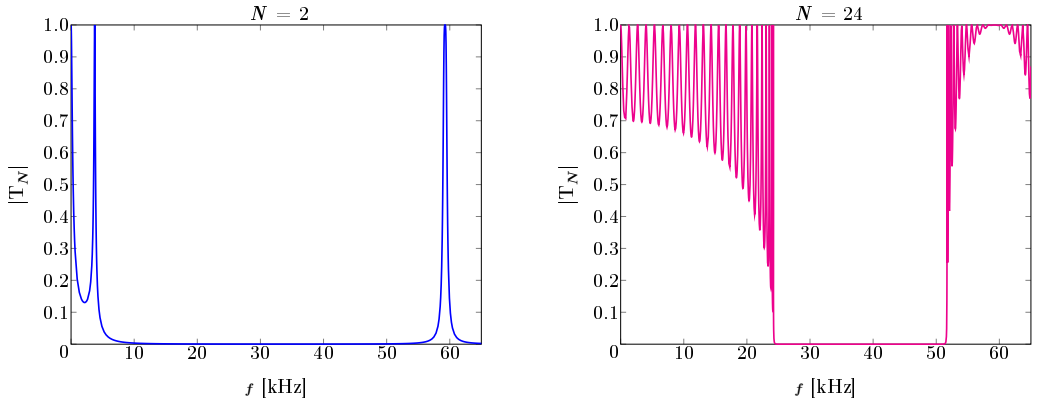

Fig. 11 Dependence of the transmission coefficient modulus on frequency for non-uniform cross-section for N=2 and N=24 cells (Ni).

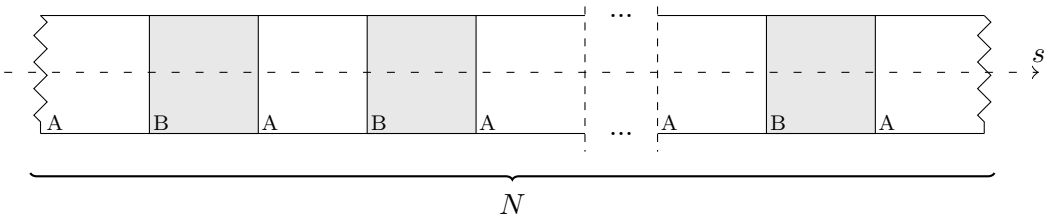

Fig. 12 An array of cells for a non-uniform mass density and Young's modulus.

The distinction of the wave numbers, Young's moduli and mass densities according to the regions is important in this case since the materials are different. The required elements of the transfer matrix then are

$$\begin{aligned} w &= e^{\mathrm{i}K_\mathrm{A}l}\left[\cos\left(K_\mathrm{B}s_1\right) + \mathrm{i}\varphi_+ \sin\left(K_\mathrm{B}s_1\right)\right] \ , \\ z &= -\mathrm{i}e^{\mathrm{i}K_\mathrm{A}l}\varphi_- \sin\left(K_\mathrm{B}s_1\right) \ , \\ \mu &= \cos\left(K_\mathrm{A}l\right)\cos\left(K_\mathrm{B}s_1\right) - \varphi_+ \sin\left(K_\mathrm{A}l\right)\sin\left(K_\mathrm{B}s_1\right) \ , \end{aligned} \tag{4.21}$$

where

$$\varphi_{\pm} = \frac{1}{2}\left(\frac{K_{\mathrm{A}}E_{\mathrm{A}}}{K_{\mathrm{B}}E_{\mathrm{B}}} \pm \frac{K_{\mathrm{B}}E_{\mathrm{B}}}{K_{\mathrm{A}}E_{\mathrm{A}}}\right), \quad K_{\mathrm{A}} = \frac{2\pi f\ell}{\sqrt{E_{\mathrm{A}}/\rho_{\mathrm{A}}}}, \quad K_{\mathrm{B}} = \frac{2\pi f\ell}{\sqrt{E_{\mathrm{B}}/\rho_{\mathrm{B}}}}. \tag{4.22}$$

The transmission coefficient of the N repeating cells can be found through

$$|\mathcal{T}_N| = \frac{1}{\sqrt{1 + \left[|\varphi_- \sin(K_{\mathrm{B}}s_1)|\, U_{N-1}(\mu)\right]^2}}. \tag{4.23}$$

Now, in contrast to the previous section, let us investigate the influence of the mass densities ratio and Young's moduli ratio on the transmission coefficient modulus dependent on frequency. There is an interest in bigger ratios of mass densities and Young's moduli. The bigger these ratios the less part of the wave is transmitted for some band. The illustration to this conclusion is shown in Fig. 13.

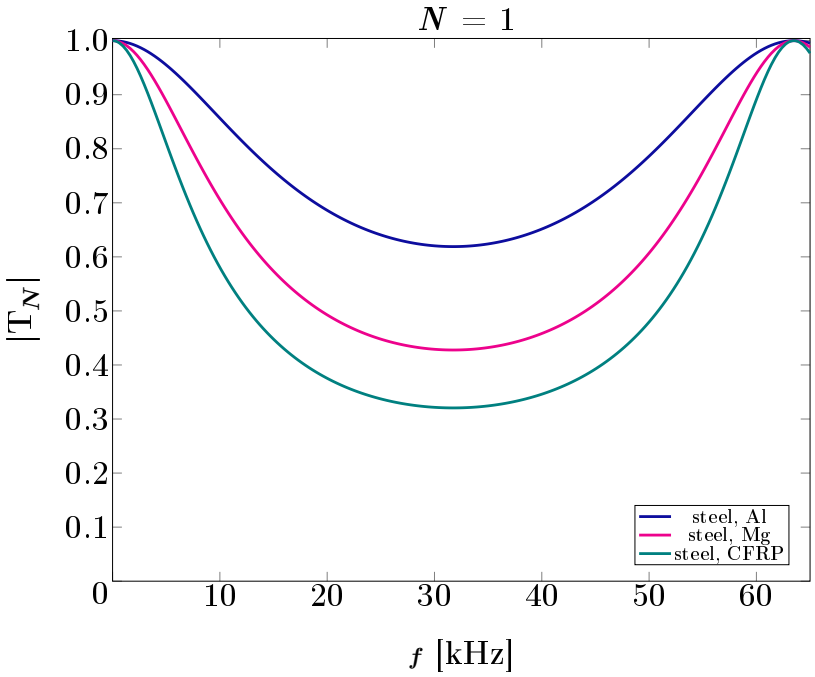

Fig. 13 Dependence of the transmission coefficient modulus on frequency for non-uniform mass density and Young's modulus for different pairs of materials.

These results are for one cell with chosen values of geometrical parameters $\ell = 1$ m, $s_1 = 4$ cm, $l = 2$ cm for steel with $\rho = 7.75$ with g/cm^3 and $E = 200$ GPa, for aluminum (Al) with $\rho = 2.7$ g/cm^3 and $E = 69$ GPa, for magnesium (Mg) with $\rho = 1.738$ g/cm^3 and $E = 45$ GPa, for carbon fiber reinforced polymer (CFRP) with $\rho = 1.4$ g/cm^3 and $E = 30$ GPa, that is the values of Kevlar Fabric CFRP. The pairs are chosen as combination of steel B and other mentioned materials A, so the approximated ratios of mass densities ρ_B/ρ_A and Young's moduli E_B/E_A accordingly are

- 2.87 and 2.9 for steel as B and Al as A,
- 4.46 and 4.44 for steel as B and Mg as A,
- 4.3 and 6.67 for steel as B and CFRP as A.

The order of materials A and B with the chosen geometrical parameters changes the transmission coefficient result. For the pairs steel and Al, steel and Mg, by changing the order of materials the transmission coefficient is the same at the beginning, but starting at some frequency the graphs are not the same, they are shifted. This fact can be seen in Fig. 14, for the pair steel and aluminum, $s_2 = 30$ cm.

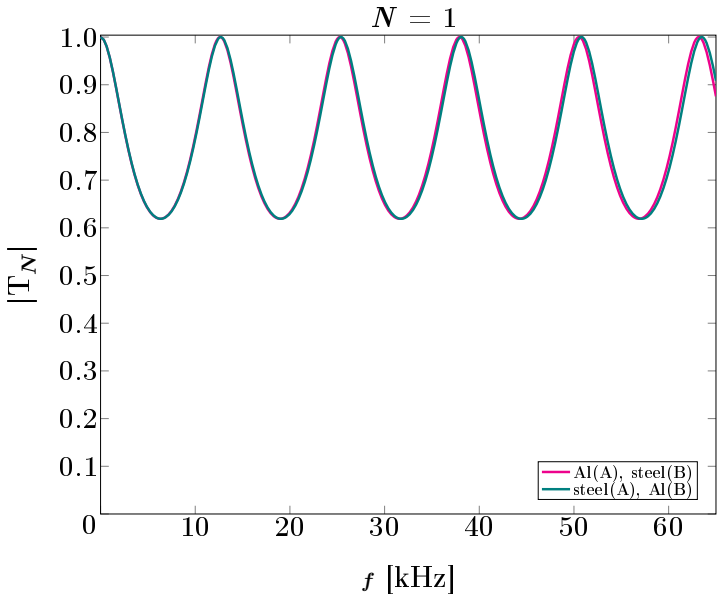

Fig. 14 Dependence of the transmission coefficient modulus on frequency for non-uniform mass density and Young's modulus for different order of materials.

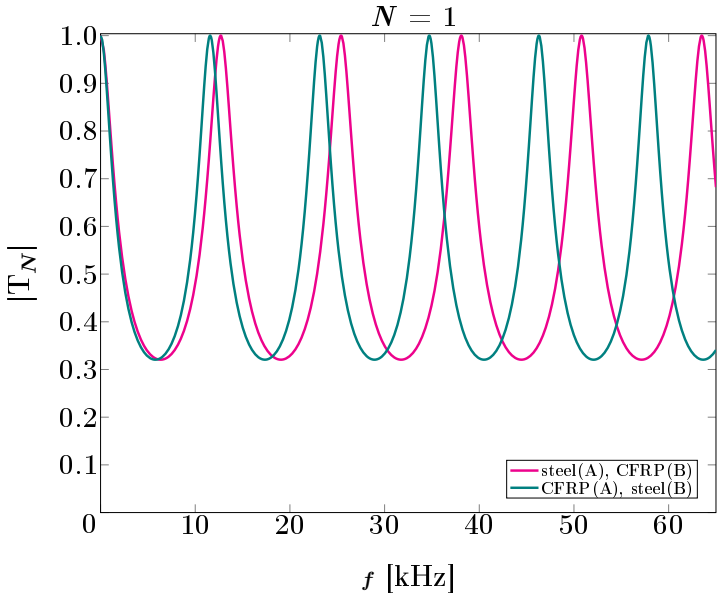

Fig. 15 Dependence of the transmission coefficient modulus on frequency for non-uniform mass density and Young's modulus for different order of materials.

For the third pair, steel and CFRP, the change of the materials' order causes the transmission coefficients differ starting from the begin of the chosen frequencies. That can be seen in Fig. 15, $s_2 = 30$ cm.

By trying different values of CRFP, i.e. mass densities and Young's moduli, it has been noticed, that the ratios should not only be bigger, but the bigger the multiplication of these ratios, the bigger amplitude can be reached. This fact is introduced in Fig. 16, $s_1 = 15$ cm and $s_2 = 30$ cm. The next types of CFRPs are chosen: E glass UD with $\rho = 1.9$ g/cm^3 and $E = 40$ GPa, E glass Fabric with $\rho = 1.9$ g/cm^3 and $E = 25$ GPa and Kevlar Fabric with $\rho = 1.4$ g/cm^3 and $E = 30$ GPa.

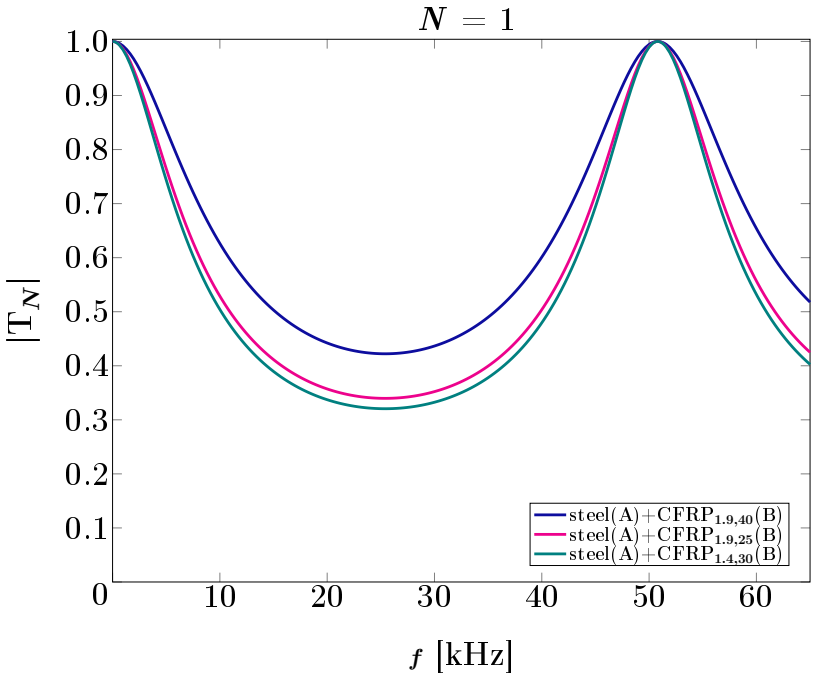

Fig. 16 Dependence of the transmission coefficient modulus on frequency for non-uniform mass density and Young's modulus for different types of CFRP.

From the graphs shown in Figs. 14 - 16 can be concluded that the order of the same chosen materials doesn't change the amplitude value.

Let us take the pairs of materials

- Al as A and steel as B, Al as A and zirconia (ZrO_2) as B,
- Al as B and steel as A, Al as B and zirconia (ZrO_2) as A.

Steel and zirconia ($\rho = 5.7$ g/cm^3 and $E = 200$ GPa) have the same Young's modulus, steel mass density is bigger than zirconia mass density, so the conclusion how the values of mass density influences the result transmission coefficients can be made (in combination with aluminum). The corresponding graphs are in Fig. 17. It can be seen, that when materials B has the same Young's modulus and material A is the same, the pair with the bigger mass density of B material will have a band gap for lower frequencies than the pair with lower B mass density (the first pair is shifted to the left from the second pair). When materials A has the same Young's modulus and material B is the same, then there is no shift for chosen values.

Let us take the pairs of materials

- Al as A and manganese (Mn) as B, Al as A and indium (In) as B,
- Al as B and manganese (Mn) as A, Al as B and indium (In) as A.

Manganese ($\rho = 7.35$ g/cm^3 and $E = 190$ GPa) and indium ($\rho = 7.35$ g/cm^3 and $E = 10$ GPa) have the same mass density, Young's modulus of manganese is bigger than Young's modulus of indium, so the conclusion how the values of Young's modulus influences the result transmission coefficients can be made (in combination with aluminum). Graphs are in Fig. 18. It can be proclaimed, that when materials B has the same mass densities and material A is the same, the pair with the smaller Young's modulus of B material produces the transmission coefficient with the higher frequency. When materials A have the same mass densities and material B is the same, then there is no shift for chosen values.

The emergence of the bang gap can be seen since $N = 4$ cells. An example of that fact is in Fig. 19. Steel and CFRP (Kevlar Fabric) are chosen. As in the case of different cross-sections,

the increase of the cells makes the angles of the band gap become the right angles, the shift of the frequency range doesn't have place. In Fig. 19 these features are shown for $N = 15$ cells.

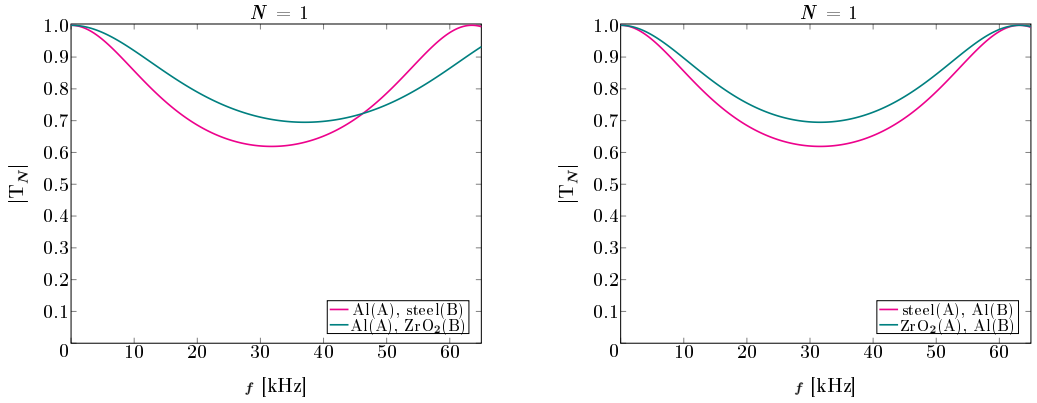

Fig. 17 Dependence of the transmission coefficient modulus on frequency for two pairs of materials, steel and ZrO_2 has the same Young's modulus.

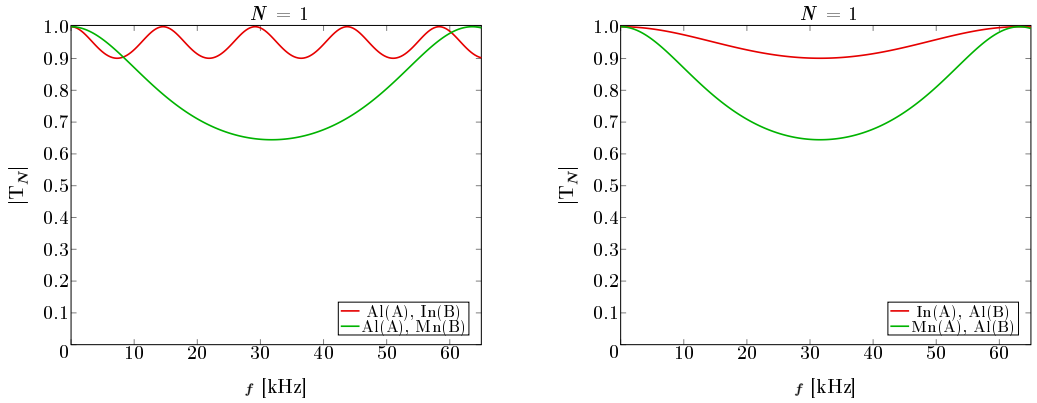

Fig. 18 Dependence of the transmission coefficient modulus on frequency for non-uniform mass density and Young's modulus for the two pairs of materials, Mn and In has the same mass density.

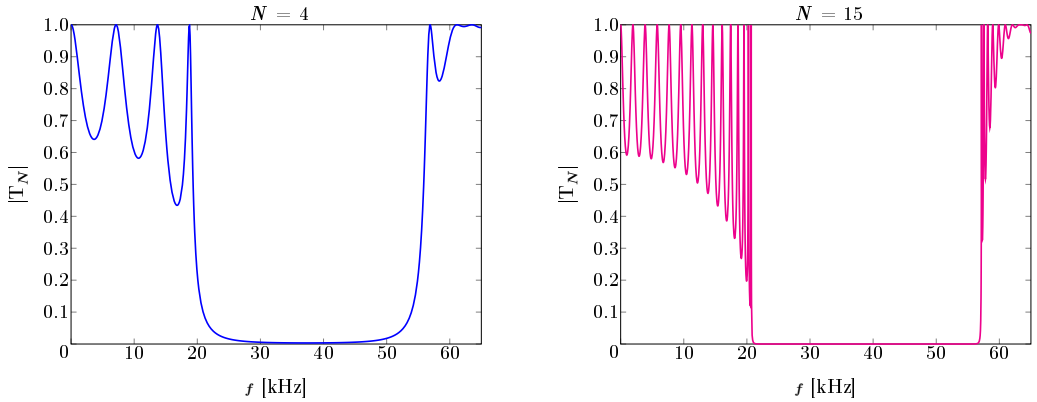

Fig. 19 Dependence of the transmission coefficient modulus for non-uniform mass density and Young's modulus on frequency for N=4 cells and N=15 cells (CFRP is A and steel is B).

5 Cell with Known Length Ratio of Its Parts

In this chapter the influence of the length ratio between two parts of the cell on the band gap existence is studied. The two types of the cells are investigated again: with the non-uniform cross-section and with with the non-uniform mass density and Young's modulus. The length ratio is included into expressions to calculate the transmission coefficient.

5.1 Single n/m Cell

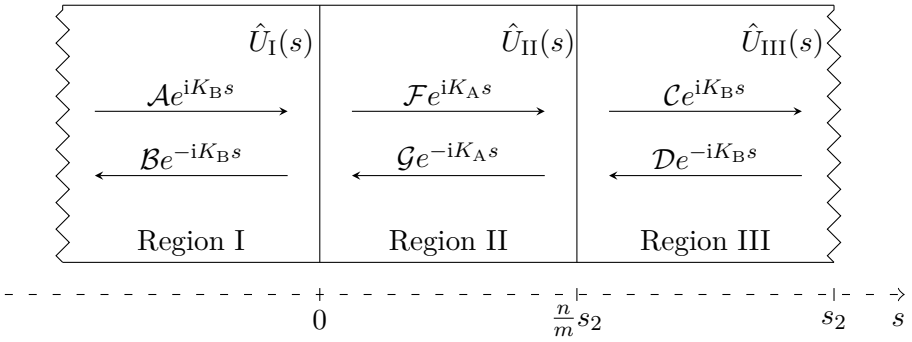

Fig. 20 Reflection and transmission of an elastic wave in a single n/m cell.

Now a cell representing a solid rod looks like in Fig. 20. The order of regions with A and B characteristics is reversed. The length ratio between two parts of the cell is represented by n/m multiplicand at the coordinate. The coordinate s_2 represents also the length of the cell, so if the whole cell consists of m parts, then Region II contributes n parts of m.

Since the order of the parts of the cell is different than in the previous chapter, the local displacement equations have the forms

$$\hat{U}_{\mathrm{I}}(s) = \mathcal{A}e^{\mathrm{i}K_{\mathrm{B}}s} + \mathcal{B}e^{-\mathrm{i}K_{\mathrm{B}}s} \,, \tag{5.1}$$

$$\hat{U}_{\mathrm{II}}(s) = \mathcal{F}e^{\mathrm{i}K_{\mathrm{A}}s} + \mathcal{G}e^{-\mathrm{i}K_{\mathrm{A}}s} \,, \tag{5.2}$$

$$\hat{U}_{\mathrm{III}}(s) = \mathcal{C}e^{\mathrm{i}K_{\mathrm{B}}s} + \mathcal{D}e^{-\mathrm{i}K_{\mathrm{B}}s} \,. \tag{5.3}$$

The balance of forces and the continuity of velocities (4.4) at the junction are applied in the same manner, but at the junctions $s = 0$ and $s = ns_2/m$ (see e.g. [1])

$$\begin{aligned} F_1 &= F_2 \,, \\ v_1 &= v_2 \,, \end{aligned} \tag{5.4}$$

where indices 1 and 2 mean two regions to the same junction.

5.1.1 Non-Uniform Cross-Section

A n/m cell with a non-uniform cross-section is sketched in Fig. 21. The unit cell itself starts at $s = 0$ and ends at $s = ns_2/m$. Here, the cross-sections in regions I and III are equal. The

material is the same in all regions, so the wave numbers K_A and K_B can be identified as K again.

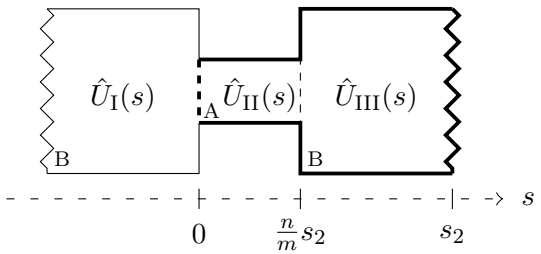

Fig. 21 A unit cell for a non-uniform cross-section.

At the points $s = 0$ and $s = ns_2/m$ the relationships between the regions then are

$$\begin{aligned}
\hat{U}_\mathrm{I}\Big|_{s=-0} &= \hat{U}_\mathrm{II}\Big|_{s=+0} \ , \\
A_\mathrm{B}\frac{\mathrm{d}\hat{U}_\mathrm{I}}{\mathrm{d}s}\Big|_{s=-0} &= A_\mathrm{A}\frac{\mathrm{d}\hat{U}_\mathrm{II}}{\mathrm{d}s}\Big|_{s=+0} \ , \\
\hat{U}_\mathrm{III}\Big|_{s=+\frac{n}{m}s_2} &= \hat{U}_\mathrm{II}\Big|_{s=-\frac{n}{m}s_2} \ , \\
A_\mathrm{B}\frac{\mathrm{d}\hat{U}_\mathrm{III}}{\mathrm{d}s}\Big|_{s=+\frac{n}{m}s_2} &= A_\mathrm{A}\frac{\mathrm{d}\hat{U}_\mathrm{II}}{\mathrm{d}s}\Big|_{s=-\frac{n}{m}s_2} \ .
\end{aligned} \tag{5.5}$$

The substitution of the points and displacement equations (5.1) - (5.3) leads to the system

$$\begin{aligned}
\mathcal{A} + \mathcal{B} &= \mathcal{F} + \mathcal{G} \ , \\
A_\mathrm{B}\left(\mathcal{A} - \mathcal{B}\right) &= A_\mathrm{A}\left(\mathcal{F} - \mathcal{G}\right) \ , \\
\mathcal{C}e^{\mathrm{i}K\frac{n}{m}s_2} + \mathcal{D}e^{-\mathrm{i}K\frac{n}{m}s_2} &= \mathcal{F}e^{\mathrm{i}K\frac{n}{m}s_2} + \mathcal{G}e^{-\mathrm{i}K\frac{n}{m}s_2} \ , \\
A_\mathrm{B}\left(\mathcal{C}e^{\mathrm{i}K\frac{n}{m}s_2} - \mathcal{D}e^{-\mathrm{i}K\frac{n}{m}s_2}\right) &= A_\mathrm{A}\left(\mathcal{F}e^{\mathrm{i}K\frac{n}{m}s_2} - \mathcal{G}e^{-\mathrm{i}K\frac{n}{m}s_2}\right) \ .
\end{aligned} \tag{5.6}$$

5.1.2 Non-Uniform Mass Density and Young's Modulus

A n/m cell with the non-uniform mass density and Young's modulus is sketched in Fig. 22. The unit cell itself starts at $s = 0$ and ends at $s = s_2$. Here, the mass densities and Young's modulus in regions I and III are equal, the cross-sections are the same in all regions.

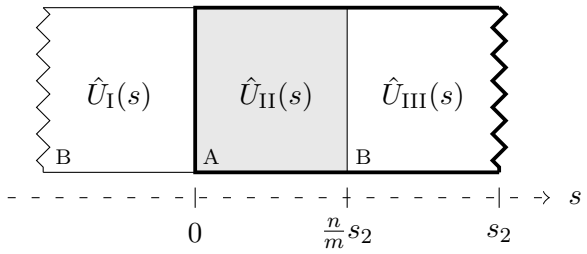

Fig. 22 A unit n/m cell for a non-uniform mass density and Young's modulus.

At points $s = 0$ and $s = ns_2/m$ the relationships between the regions are

$$\begin{aligned} \hat{U}_{\mathrm{I}}\Big|_{s=-0} &= \hat{U}_{\mathrm{II}}\Big|_{s=+0} \ , \\ E_{\mathrm{B}}\frac{\mathrm{d}\hat{U}_{\mathrm{I}}}{\mathrm{d}s}\Big|_{s=-0} &= E_{\mathrm{A}}\frac{\mathrm{d}\hat{U}_{\mathrm{II}}}{\mathrm{d}s}\Big|_{s=+0} \ , \\ \hat{U}_{\mathrm{III}}\Big|_{s=+\frac{n}{m}s_2} &= \hat{U}_{\mathrm{II}}\Big|_{s=-\frac{n}{m}s_2} \ , \\ E_{\mathrm{B}}\frac{\mathrm{d}\hat{U}_{\mathrm{III}}}{\mathrm{d}s}\Big|_{s=+\frac{n}{m}s_2} &= E_{\mathrm{A}}\frac{\mathrm{d}\hat{U}_{\mathrm{II}}}{\mathrm{d}s}\Big|_{s=-\frac{n}{m}s_2} \ . \end{aligned} \tag{5.7}$$

The substitution of the points and displacement equations (5.1) - (5.3) leads to the system

$$\begin{aligned} \mathcal{A} + \mathcal{B} &= \mathcal{F} + \mathcal{G} \ , \\ E_{\mathrm{B}}K_{\mathrm{B}}\left(\mathcal{A} - \mathcal{B}\right) &= E_{\mathrm{A}}K_{\mathrm{A}}\left(\mathcal{F} - \mathcal{G}\right) \ , \\ \mathcal{C}e^{\mathrm{i}K_{\mathrm{B}}\frac{n}{m}s_2} + \mathcal{D}e^{-\mathrm{i}K_{\mathrm{B}}\frac{n}{m}s_2} &= \mathcal{F}e^{\mathrm{i}K_{\mathrm{A}}\frac{n}{m}s_2} + \mathcal{G}e^{-\mathrm{i}K_{\mathrm{A}}\frac{n}{m}s_2} \ , \\ E_{\mathrm{B}}K_{\mathrm{B}}\left(\mathcal{C}e^{\mathrm{i}K_{\mathrm{B}}\frac{n}{m}s_2} - \mathcal{D}e^{-\mathrm{i}K_{\mathrm{B}}\frac{n}{m}s_2}\right) &= E_{\mathrm{A}}K_{\mathrm{A}}\left(\mathcal{F}e^{\mathrm{i}K_{\mathrm{A}}\frac{n}{m}s_2} - \mathcal{G}e^{-\mathrm{i}K_{\mathrm{A}}\frac{n}{m}s_2}\right) \ . \end{aligned} \tag{5.8}$$

5.2 Multiple Cells of *n*/*m* Type

Considering the result from the previous chapter, that with the increasing number of cells for a given set of parameters, the band gaps become more pronounced, let us see how the choice of the n and m influences the behavior of band gaps.

5.2.1 Multiple *n*/*m* Cells

The multiple n/m cells solid rods are shown in Fig. 23 and Fig. 29. The transfer matrix, the point at which the Chebyshev polynomials are evaluated and the transmission coefficient of N cells are a little bit different than in Section 4.2, since the order of A and B regions are reversed

$$\mathbf{M}_N = \begin{pmatrix} e^{-\mathrm{i}K_{\mathrm{B}}Ns_2}\left[U_N(\mu) - w^* e^{-\mathrm{i}K_{\mathrm{B}}s_2}U_{N-1}(\mu)\right] & ze^{-\mathrm{i}K_{\mathrm{B}}(N-1)s_2}U_{N-1}(\mu) \\ z^* e^{\mathrm{i}K_{\mathrm{B}}(N-1)s_2}U_{N-1}(\mu) & e^{\mathrm{i}K_{\mathrm{B}}Ns_2}\left[U_N(\mu) - we^{\mathrm{i}K_{\mathrm{B}}s_2}U_{N-1}(\mu)\right] \end{pmatrix} \ , \tag{5.9}$$

$$\mu = \frac{1}{2}\left(we^{\mathrm{i}K_{\mathrm{B}}s_2} + w^* e^{-\mathrm{i}K_{\mathrm{B}}s_2}\right) \ , \tag{5.10}$$

$$|\mathcal{T}_N| = \frac{1}{\sqrt{1 + \left[|z|\,U_{N-1}(\mu)\right]^2}} \ . \tag{5.11}$$

Elements w and z will be expressed for each case separately. Their expressions are almost the same as was derived earlier. The difference is in the reverse of wave numbers K_{A} and K_{B} and use of expression $1 - n/m$ instead of l.

5.2.1.1 Non-Uniform Cross-Section

The solid rod consisting of N multiple cells, where the single cell consists of the two parts with different cross-sections with the given length ratio of these parts, is sketched in Fig. 23.

The needed expressions are

$$\begin{aligned} w &= e^{\mathrm{i}K\left(1-\frac{n}{m}\right)s_2}\left[\cos\left(K\frac{n}{m}s_2\right) + \mathrm{i}\varphi_+ \sin\left(K\frac{n}{m}s_2\right)\right] \ , \\ z &= \mathrm{i}e^{\mathrm{i}K\left(1-\frac{n}{m}\right)s_2}\varphi_- \sin\left(K\frac{n}{m}s_2\right) \ , \\ \mu &= \cos\left(K\left(1-\frac{n}{m}\right)s_2\right)\cos\left(K\frac{n}{m}s_2\right) - \phi_+ \sin\left(K\left(1-\frac{n}{m}\right)s_2\right)\sin\left(K\frac{n}{m}s_2\right) \ , \end{aligned} \tag{5.12}$$

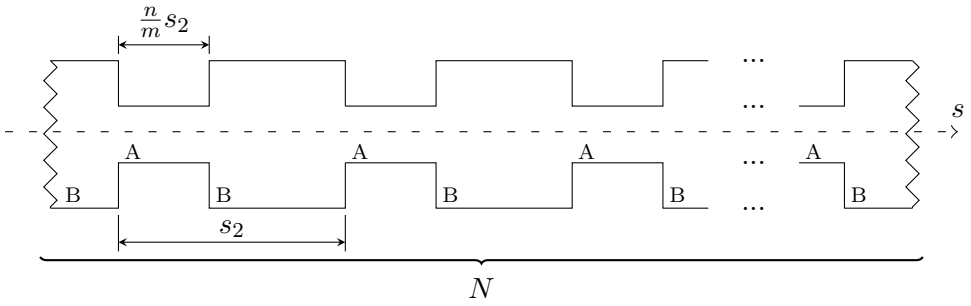

Fig. 23 Multiple n/m cells for a non-uniform cross-section.

where

$$\phi_{\pm} = \frac{1}{2}\left(\frac{A_{\mathrm{A}}}{A_{\mathrm{B}}} \pm \frac{A_{\mathrm{B}}}{A_{\mathrm{A}}}\right) , \quad A_{\mathrm{A}} = \pi r_{\mathrm{A}}^2 , \quad A_{\mathrm{B}} = \pi r_{\mathrm{B}}^2 , \quad K = \frac{2\pi f \ell}{\sqrt{E/\rho}} . \tag{5.13}$$

The transmission coefficient can be found through

$$|\mathcal{T}_N| = \frac{1}{\sqrt{1 + \left[\left|\phi_- \sin\left(K\frac{n}{m}s_2\right)\right| U_{N-1}(\mu)\right]^2}} . \tag{5.14}$$

Based on the results from the previous chapter let us find out the regularities for this type of the cell.

In Fig. 24 there are the graphs for the solid rod consisted of the two aluminum cells, the number of parts is $m = 10$, the radii have values $r_{\mathrm{A}} = 1$ cm and $r_{\mathrm{B}} = 10$ cm, the length of one cell is 10 cm.

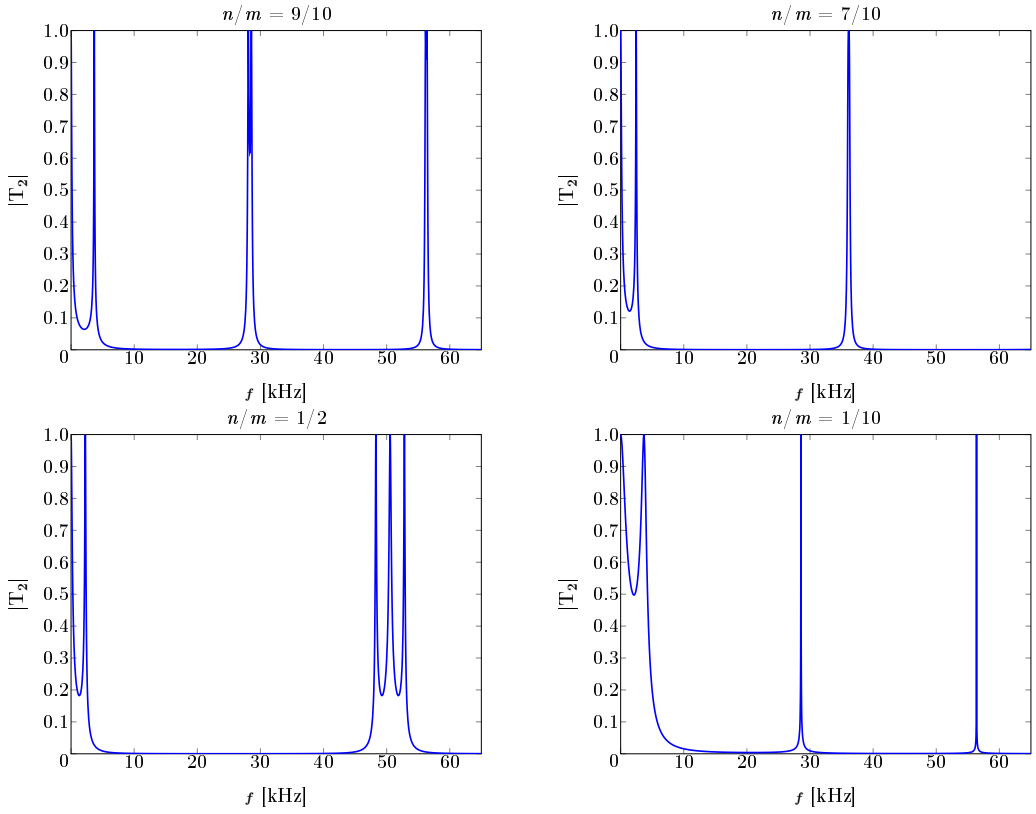

Fig. 24 Dependence of the transmission coefficient modulus on frequency for non-uniform cross-sections of different lengths and $N = 2$ repeating cells (aluminum).

The first part of the transmission coefficient graphs represented in Fig. 24 is the drop, the second part is the 1st band gap. The following part differs for chosen value n of m. Can be concluded that for $n \geq m/2$ and n is closer to m the 1st band gap is wider, the widest one is when the lengths of both cell parts are equal. The 1st band gap is followed by the drop or the band gap. The 1st drop amplitude is bigger for bigger n. All drops can be divided into two groups: *side drops* and *internal drops*. For $n > m/2$ there are both types of drops, but for $n \leq m/2$ there are only side drops. For $n < m/2$ the 1st band gap is narrower, the 1st drop amplitude is smaller.

Let us have a look at Fig. 25 and Fig. 26, where the wider spectrum is chosen, it can be seen, that if n equals to e.g. 3 and 7 or 1 and 9 (their sum equals to m), then there is a full transmission of the wave almost at the same frequencies. Also it can be noticed that the band gaps are trying to form some groups dependent on the values of n and m. The length s_2 is set to 2 cm.

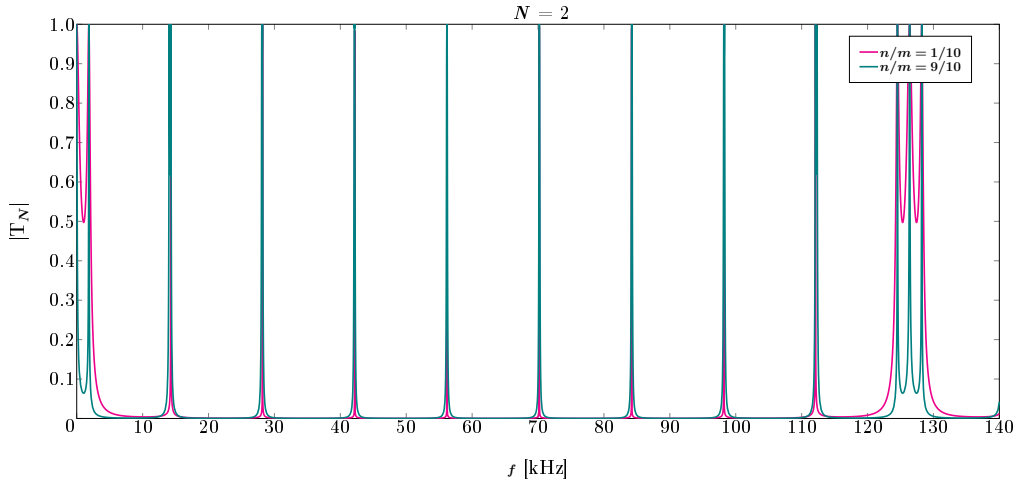

Fig. 25 Dependence of the transmission coefficient modulus on frequency for non-uniform cross-sections from aluminum with $n/m = 1/10$ and $n/m = 9/10$ for two cells ($s_2 = 10$ cm).

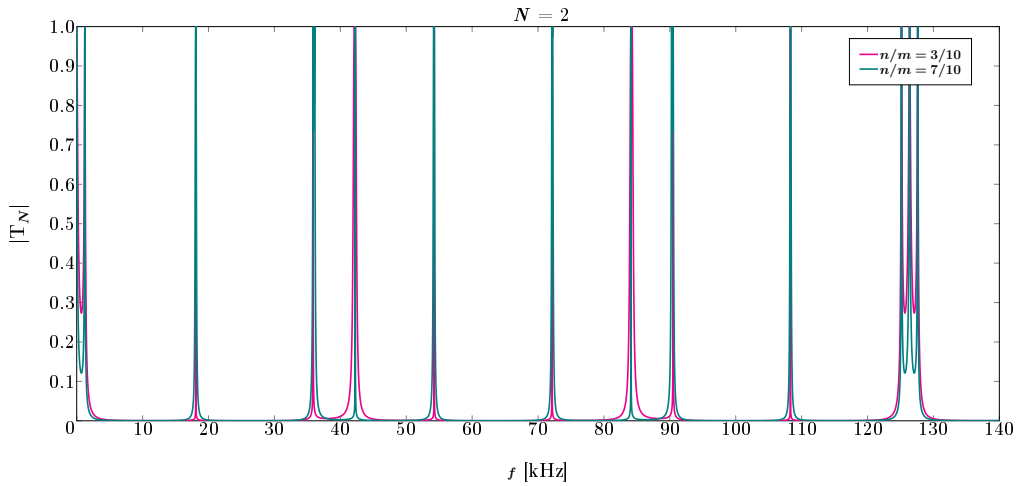

Fig. 26 Dependence of the transmission coefficient modulus on frequency for non-uniform cross-sections from aluminum with $n/m = 3/10$ and $n/m = 7/10$ for two cells ($s_2 = 10$ cm).

Now it is easily to get and see very clearly the property: the length of the cell is less, the band gap is wider. To be more precise the band gap is wider almost as much times as s_2 was made

less, because there is a shift of the full transmission frequencies, forming the band gap borders, to the right and to the left accordingly proportional to the number of times. This property can be seen in Fig. 27, where the length s_2 is remained to be 10 cm for one curve and 5 cm for the other one, the both parts of the cell have equal lengths, i.e. $n/m = 1/2$. The symmetry of the curves can be noticed.

In Fig. 28 two number of cells' repetitions are chosen: $N = 2$ and $N = 7$. The length of one cell is $s_2 = 5$ cm with the length ratio $n/m = 1/2$ is remained. By adding more repetitions the band gap borders become more straight rather rounded and are a bit shifted.

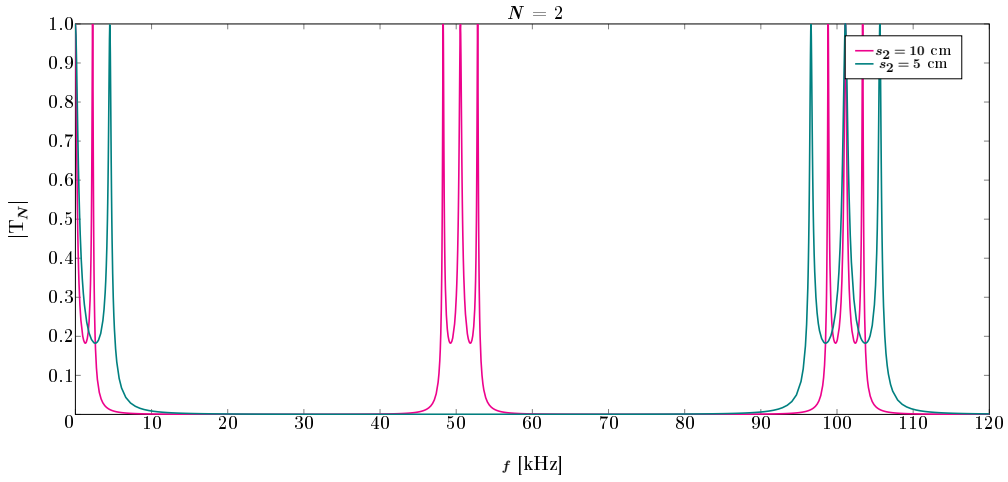

Fig. 27 Dependence of the transmission coefficient modulus on frequency for non-uniform cross-sections with different s_2 length and $n/m = 1/2$.

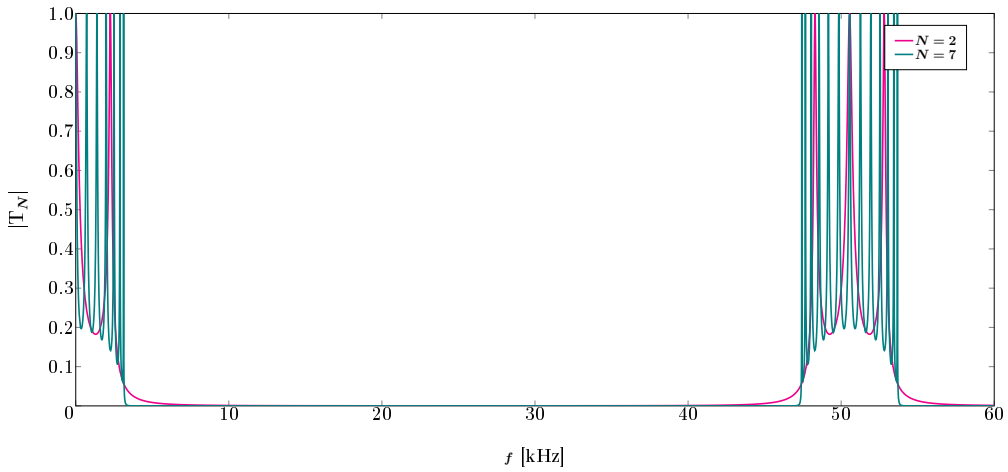

Fig. 28 Dependence of the transmission coefficient modulus on frequency for non-uniform cross-sections with $N = 2$ and $N = 7$ ($s_2 = 5$ cm, $n/m = 1/2$).

5.2.1.2 Non-Uniform Density and Young's Modulus

The solid rod consisting of N multiple cells, where the single cell consists of the two parts with different mass densities and Young's modulus with the given length ratio of these parts, is shown in Fig. 29.

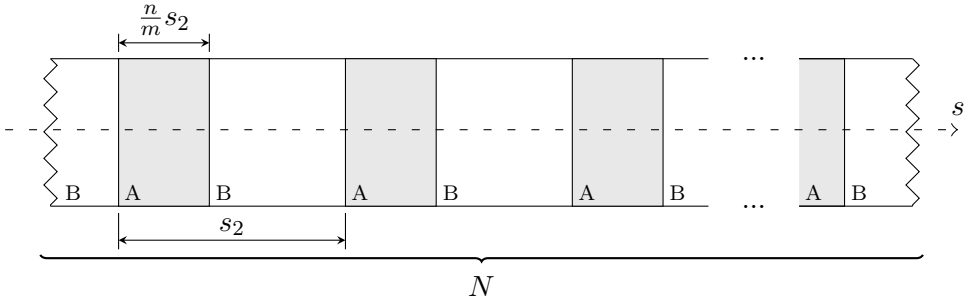

Fig. 29 Multiple n/m cells for a non-uniform mass density and Young's modulus.

The needed expressions are

$$\begin{aligned} w &= e^{\mathrm{i}K_\mathrm{B}\left(1-\frac{n}{m}\right)s_2}\left[\cos\left(K_\mathrm{A}\frac{n}{m}s_2\right)+\mathrm{i}\varphi_+\sin\left(K_\mathrm{A}\frac{n}{m}s_2\right)\right]\,,\\ z &= \mathrm{i}e^{\mathrm{i}K_\mathrm{B}\left(1-\frac{n}{m}\right)s_2}\varphi_-\sin\left(K_\mathrm{A}\frac{n}{m}s_2\right)\,,\\ \mu &= \cos\left(K_\mathrm{B}\left(1-\frac{n}{m}\right)s_2\right)\cos\left(K_\mathrm{A}\frac{n}{m}s_2\right)-\varphi_+\sin\left(K_\mathrm{B}\left(1-\frac{n}{m}\right)s_2\right)\sin\left(K_\mathrm{A}\frac{n}{m}s_2\right)\,, \end{aligned} \tag{5.15}$$

where

$$\varphi_\pm=\frac{1}{2}\left(\frac{K_\mathrm{A}E_\mathrm{A}}{K_\mathrm{B}E_\mathrm{B}}\pm\frac{K_\mathrm{B}E_\mathrm{B}}{K_\mathrm{A}E_\mathrm{A}}\right)\,,\quad K_\mathrm{A}=\frac{2\pi f\ell}{\sqrt{E_\mathrm{A}/\rho_\mathrm{A}}}\,,\quad K_\mathrm{B}=\frac{2\pi f\ell}{\sqrt{E_\mathrm{B}/\rho_\mathrm{B}}}\,. \tag{5.16}$$

The transmission coefficient can be found through

$$|\mathcal{T}_N|=\frac{1}{\sqrt{1+\left[\left|\varphi_-\sin\left(K_\mathrm{A}\frac{n}{m}s_2\right)\right|U_{N-1}(\mu)\right]^2}}\,. \tag{5.17}$$

Based on the results from the previous chapter let us find out the regularities for this type of the cell.

In Fig. 30 there are the graphs for the solid rod consisted of four cells. One cell of which is represented by the pair of CFRP (Kevlar Fabric) as material A and steel as material B. The length of one cell is 10 cm, the number of parts is $m = 10$, n is taken different. In comparison to the cell of the non-uniform cross-section, this type of the cell with the chosen parameters' values needs more repetitions, because for $N = 4$ the band gap is seen, but the 4th drop is not a band gap for every chosen n.

The widest band gap is when the lengths of both cell parts are equal, the start of the band gap in this case is the first one in comparison to the other chosen values of n and m, see Fig. 31. Also it can be noticed that in comparison to the case of different cross-sections, in the case of the different mass densities and Young's moduli the sum of two n being equal to m doesn't lead to the full transmission at the same frequencies for all such pairs. It can bee seen that it is almost true for the pair $n = 7$ and $n = 3$, but not for the pair $n = 9$ and $n = 1$, where $m = 10$.

From the previous chapter, it is known that the order of materials influences the frequency of the transmission coefficient modulus when the parts of the cell have the same length. But what will happen if the order of materials is changed in case of different n from m? The blue plots represent the same combination of steel as B and CFRP as A, the new magenta color represents the reversed order of materials, so steel is A and CFRP is B in Fig. 32. By adjusting the values of n from m and changing the order of materials it is possible to shift the range of the band gaps and influence the widths of these band gaps.

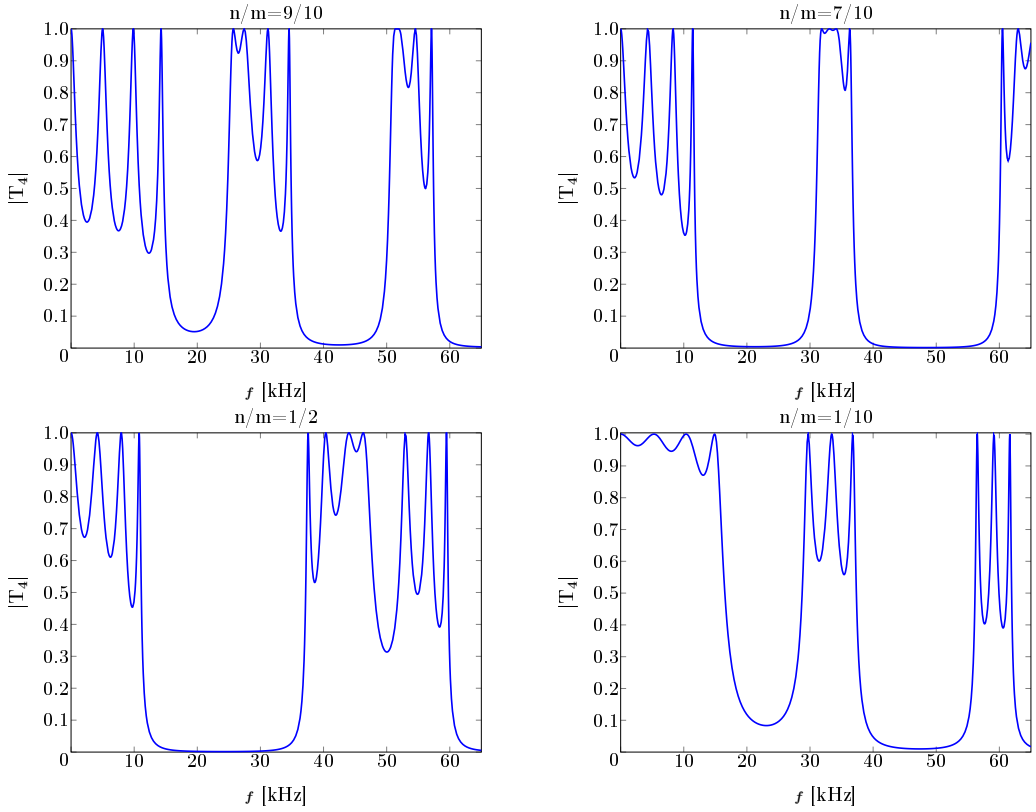

Fig. 30 Dependence of the transmission coefficient modulus on frequency for non-uniform mass density and Young's modulus for four n/m repeating cells. CFRP is A and steel is B.

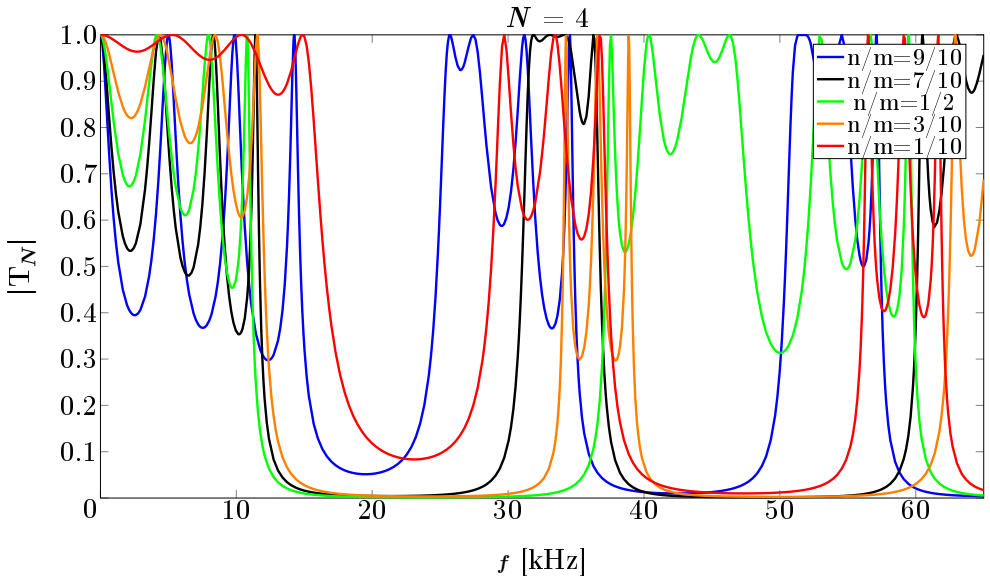

Fig. 31 Dependence of the transmission coefficient modulus on frequency for non-uniform mass density and Young's modulus for four n/m repeating cells (CFRP is A and steel is B) with different values of n.

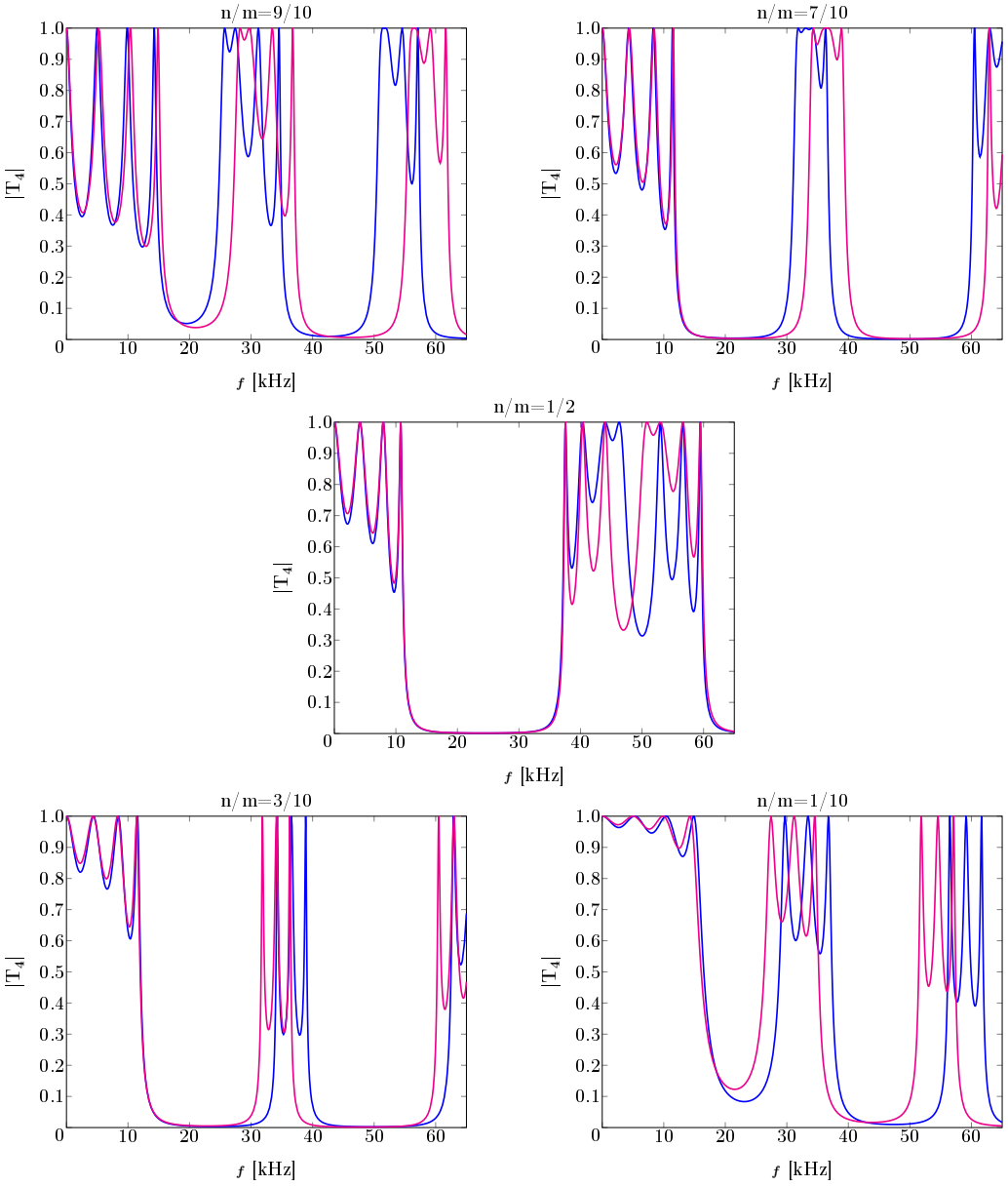

Fig. 32 Dependence of the transmission coefficient modulus on frequency for non-uniform mass density and Young's modulus for four n/m repeating cells. CFRP (A) and steel (B) are in blue, steel (A) and CFRP (B) are in magenta.

6 Propagation of Elastic Waves through Linearly Graded Material

In this chapter the solid rode consisted of the inhomogeneous region is considered. The inhomogeneity is represented by the linear Young's modulus change. The positive and negative gradients are investigated, their combination, form the triangular profile of Young's modulus, is also analyzed. The solution of model equation describing the propagation through the linearly graded region is derived.

6.1 Model Equation and its Solution

Let us consider the solid rode as sketched in Fig. 33, fabricated from two materials M_{I} and M_{II}. There is an inhomogeneous region of the length of ℓ between these two regions.

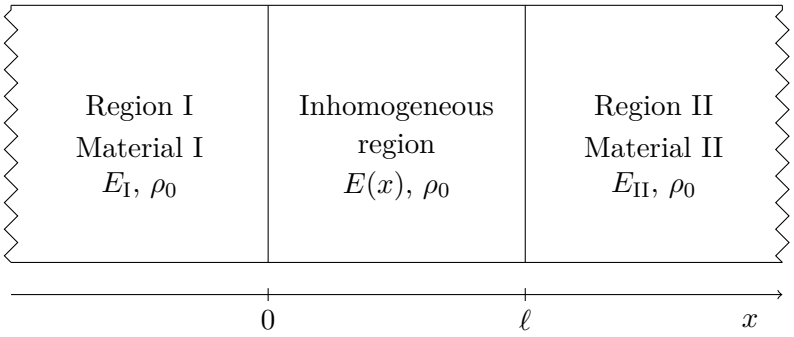

Fig. 33 Distribution of the regions in a solid rode.

The inhomogeneity of material properties can be caused by the temperature, for example. If the solid rode is heated in such a way that there is a large variation in temperature along the solid rode length, Young's modulus E depends on x since Young's modulus is known to be sensitive to the large temperature changes. However, in such cases mass density ρ_0 varies only little, so that it is possible to assume that it remains constant (see e.g. [10]). Young's modulus then can be described as a function of the material properties and volume fractions of consistent materials (see e.g. [11])

$$E = E_{\mathrm{I}} V_{\mathrm{I}} + E_{\mathrm{II}} V_{\mathrm{II}} \,, \tag{6.1}$$

where E_{I} and E_{II} denote Young's moduli of the supposed materials and V_{I} and V_{II} are the volume fractions of the constituent materials that satisfy the following condition

$$V_{\mathrm{I}} + V_{\mathrm{II}} = 1 \,. \tag{6.2}$$

Let us make an assumption that the material composition in an inhomogeneous region varies continuously only along the x-axis, then let us denote $V_{\mathrm{II}} = V(x)$ and on the basis of Eq. (6.2) can be written $V_{\mathrm{I}} = 1 - V(x)$. Then Eq. (6.1) can be written as

$$E(x) = E_{\mathrm{II}} V(x) + E_{\mathrm{I}}[1 - V(x)] \,, \tag{6.3}$$

The material composition in the solid rode inhomogeneous region is supposed to be distributed according to the following linear law

$$V(x) = \frac{x}{\ell} \,, \tag{6.4}$$

where ℓ is considered as a characteristic length.

With respect to Eqs. (6.3) and (6.4) Young's modulus can be expressed as

$$E(x) = E_{\mathrm{II}}\frac{x}{\ell} + E_{\mathrm{I}}\left(1 - \frac{x}{\ell}\right) = E_{\mathrm{I}} + (E_{\mathrm{II}} - E_{\mathrm{I}})\,\frac{x}{\ell}\ . \tag{6.5}$$

There is a derivation of equation describing the propagation of elastic waves in a solid rode written in dimensionless form in Chapter 3. Let us repeat equation (3.12) again

$$\frac{\mathrm{d}^2\hat{U}(s)}{\mathrm{d}s^2} + \frac{1}{\eta(s)}\frac{\mathrm{d}\eta(s)}{\mathrm{d}s}\frac{\mathrm{d}\hat{U}(s)}{\mathrm{d}s} + \frac{1}{S(s)}\frac{\mathrm{d}S(s)}{\mathrm{d}s}\frac{\mathrm{d}\hat{U}(s)}{\mathrm{d}s} + \frac{\xi(s)}{\eta(s)}K^2\hat{U}(s) = 0\ , \tag{6.6}$$

where

$$\begin{aligned} &s = \frac{x}{\ell}\ , \qquad \hat{U}(s) = \frac{\hat{u}(s)}{\ell}\ , \qquad S(s) = \frac{A(s)}{\ell^2}\ , \qquad \eta(s) = \frac{E(s)}{E_0}\ , \\ &\xi(s) = \frac{\rho(s)}{\rho_0}\ , \qquad K^2 = \frac{\omega^2\ell^2}{c_{L0}^2}\ , \qquad c_{L0} = \sqrt{\frac{E_0}{\rho_0}}\ . \end{aligned} \tag{6.7}$$

The third term in Eq. (6.6) can be omitted since the cross-section is considered to be constant in this chapter. Young's modulus E_0 is replaced by E_{I} according to the notations, then

$$\eta(s) = \frac{E(s)}{E_{\mathrm{I}}}\ , \quad K_{\mathrm{I}}^2 = \frac{\omega^2\ell^2}{c_{L1}^2}\ , \quad c_{L1} = \sqrt{\frac{E_{\mathrm{I}}}{\rho_0}}. \tag{6.8}$$

The dimensionless form of Young's modulus, expressed by Eq. (6.5), and dimensionless mass density are

$$\eta(a;s) = \frac{E(s)}{E_{\mathrm{I}}} = 1 + \frac{E_{\mathrm{II}} - E_{\mathrm{I}}}{E_{\mathrm{I}}}s = 1 + as\ , \tag{6.9}$$

$$\xi(s) = \frac{\rho(s)}{\rho_0} = 1\ . \tag{6.10}$$

After the substitution into Eq. (6.6) expressions (6.8) - (6.10), the longitudinal propagation of elastic waves through a continuously inhomogeneous solid rode can be described as (see e.g. [10])

$$\frac{\mathrm{d}^2\hat{U}(s)}{\mathrm{d}s^2} + \frac{1}{\eta(a;s)}\frac{\mathrm{d}\eta(a;s)}{\mathrm{d}s}\frac{\mathrm{d}\hat{U}(s)}{\mathrm{d}s} + \frac{\omega^2\ell^2}{c_L^2}\hat{U}(s) = 0\ , \tag{6.11}$$

where $c_L = \sqrt{E(s)/\rho_0}$.

Let us substitute the expressions related to the dimensionless Young's modulus into Eq. (6.11)

$$\frac{\mathrm{d}^2\hat{U}(s)}{\mathrm{d}s^2} + \frac{a}{1+as}\frac{\mathrm{d}\hat{U}(s)}{\mathrm{d}s} + \frac{\omega^2\ell^2\rho_0}{(1+as)E_{\mathrm{I}}}\hat{U}(s) = 0\ . \tag{6.12}$$

The third term can be expressed through the wave number K_{I}, so Eq. (6.12) can be written as

$$\frac{\mathrm{d}^2\hat{U}(s)}{\mathrm{d}s^2} + \frac{a}{1+as}\frac{\mathrm{d}\hat{U}(s)}{\mathrm{d}s} + \frac{K_{\mathrm{I}}^2}{1+as}\hat{U}(s) = 0\ . \tag{6.13}$$

The solution of the above differential equation is

$$\hat{U}(s) = C_1\mathrm{J}_0\left(2K_{\mathrm{I}}\frac{\sqrt{1+as}}{|a|}\right) + C_2\mathrm{Y}_0\left(2K_{\mathrm{I}}\frac{\sqrt{1+as}}{|a|}\right)\ , \tag{6.14}$$

where C_1 and C_2 are complex integration constants, J_0 and Y_0 are the Bessel functions of the first and second kinds of order zero.

6.2 Linear Gradients of Young's Modulus

Let us define more exactly the solution of the model equation describing propagation of elastic waves through the linearly graded material for the cases with positive and negative gradients of Young's modulus. Analogically to the previous cases let us use notations A and B for different regions, but subscript B corresponds to the higher value of Young's modulus, A to the lower one. It follows

$$E_{\mathrm{B}} > E_{\mathrm{A}} \ . \tag{6.15}$$

6.2.1 Positive Linear Gradient of Young's Modulus

The solution of the model equation (6.14) with the positive linear gradient of Young's modulus has the form

$$\hat{U}_{\mathrm{AB}}(s) = C_1 \mathrm{J}_0\left(2K_{\mathrm{A}}\frac{\sqrt{1+as}}{a}\right) + C_2 \mathrm{Y}_0\left(2K_{\mathrm{A}}\frac{\sqrt{1+as}}{a}\right) \ , \tag{6.16}$$

where subscript AB means the change of Young's modulus from the lower value to higher, the corresponding wave numbers have subscripts A and B. The expression for a, based on (6.10), is

$$a = \frac{E_{\mathrm{B}} - E_{\mathrm{A}}}{E_{\mathrm{A}}} \ . \tag{6.17}$$

The derivation of equation (6.16) is

$$\frac{\mathrm{d}\hat{U}_{\mathrm{AB}}}{\mathrm{d}s} = -\frac{K_{\mathrm{A}}}{\sqrt{1+as}}\left[C_1 \mathrm{J}_1\left(2K_{\mathrm{A}}\frac{\sqrt{1+as}}{a}\right) + C_2 \mathrm{Y}_1\left(2K_{\mathrm{A}}\frac{\sqrt{1+as}}{a}\right)\right] \ , \tag{6.18}$$

where J_1 and Y_1 are the Bessel functions of the first and second kinds of order one.

6.2.2 Negative Linear Gradient of Young's Modulus

The coefficient a defined by (6.10) is negative in this case. The needed Bessel functions of the first and second kind of the negative argument can be found through the formulas (see e.g. [12], [13])

$$\begin{aligned} \mathrm{J}_{\mathrm{n}}(-z) &= (-1)^{\mathrm{n}} \mathrm{J}_{\mathrm{n}}(z) \ , \\ \mathrm{Y}_{\mathrm{n}}(-z) &= (-1)^{\mathrm{n}} \left[\mathrm{Y}_{\mathrm{n}}(z) + \mathrm{i}2\mathrm{J}_{\mathrm{n}}(z)\right] \ , \end{aligned} \tag{6.19}$$

where n is integer.

The solution of model equation (6.14) with the negative linear gradient of Young's modulus has the form

$$\hat{U}_{\mathrm{BA}}(s) = C_3 \mathrm{J}_0\left(2K_{\mathrm{B}}\frac{\sqrt{1-bs}}{b}\right) + C_4\left[\mathrm{Y}_0\left(2K_{\mathrm{B}}\frac{\sqrt{1-bs}}{b}\right) + \mathrm{i}2\mathrm{J}_0\left(2K_{\mathrm{B}}\frac{\sqrt{1-bs}}{b}\right)\right] \ , \tag{6.20}$$

where

$$b = \frac{E_{\mathrm{B}} - E_{\mathrm{A}}}{E_{\mathrm{B}}} \ . \tag{6.21}$$

The derivation of equation (6.20) is

$$\begin{aligned} &\frac{\mathrm{d}\hat{U}_{\mathrm{BA}}}{\mathrm{d}s} = \\ &\quad \frac{K_{\mathrm{B}}}{\sqrt{1-bs}}\left(C_3 \mathrm{J}_1\left(2K_{\mathrm{B}}\frac{\sqrt{1-bs}}{b}\right) + C_4\left[\mathrm{Y}_1\left(2K_{\mathrm{B}}\frac{\sqrt{1-bs}}{b}\right) + \mathrm{i}2\mathrm{J}_1\left(2K_{\mathrm{B}}\frac{\sqrt{1-bs}}{b}\right)\right]\right) \ . \end{aligned} \tag{6.22}$$

6.3 One Cell

Let us form the transfer matrix of one cell representing the part of the solid rode consisted of the graded material.

6.3.1 Boundary Conditions

Let us assume the solid rode as sketched in Fig. 34.

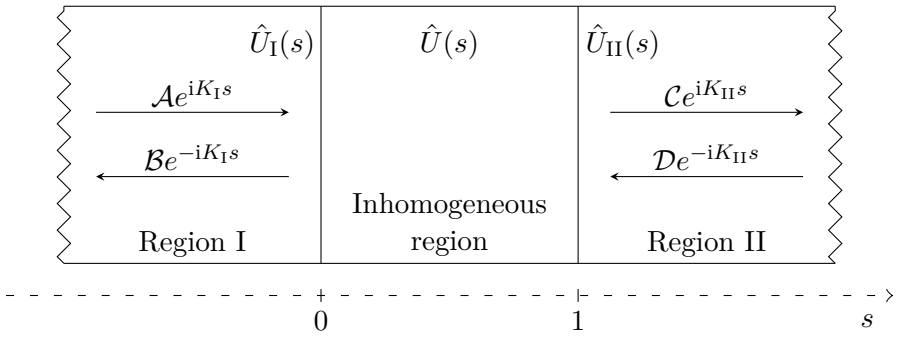

Fig. 34 Reflection and transmission of an elastic wave in an inhomogeneous region.

The notation is dimensionless, the inhomogeneous region starts at $s = 0$ and ends at $s = 1$. The wave propagates from the left to the right, the dimensionless notations for the local displacements in the corresponding regions are marked and they can be expressed as

$$\hat{U}_{\mathrm{I}}(s) = \mathcal{A}e^{\mathrm{i}K_{\mathrm{I}}s} + \mathcal{B}e^{-\mathrm{i}K_{\mathrm{I}}s} \,, \tag{6.23}$$

$$\hat{U}(s) = \hat{U}_{\mathrm{AB}}(s) \quad \text{or} \quad \hat{U}(s) = \hat{U}_{\mathrm{BA}}(s) \,, \tag{6.24}$$

$$\hat{U}_{\mathrm{II}}(s) = \mathcal{C}e^{\mathrm{i}K_{\mathrm{II}}s} + \mathcal{D}e^{-\mathrm{i}K_{\mathrm{II}}s} \,, \tag{6.25}$$

where the wave number of the second region is

$$K_{\mathrm{II}}^2 = \frac{\omega^2 \ell^2}{c_{L2}^2} \,, \quad c_{L2} = \sqrt{\frac{E_{\mathrm{II}}}{\rho_0}}. \tag{6.26}$$

The boundary conditions at the junctions of regions can be found in the same way as were done in the previous cases (see e.g. [1]), by taking into account the balance of forces and the continuity of velocities at the junctions $s = 0$ and $s = 1$. That can be written as

$$\begin{aligned} \hat{U}_{\mathrm{I}}\Big|_{s=-0} &= \hat{U}\Big|_{s=+0} \,, \\ \frac{\mathrm{d}\hat{U}_{\mathrm{I}}}{\mathrm{d}s}\Big|_{s=-0} &= \frac{\mathrm{d}\hat{U}}{\mathrm{d}s}\Big|_{s=+0} \,, \\ \hat{U}_{\mathrm{II}}\Big|_{s=+1} &= \hat{U}\Big|_{s=-1} \,, \\ E_{\mathrm{II}} \, \frac{\mathrm{d}\hat{U}_{\mathrm{II}}}{\mathrm{d}s}\Big|_{s=+1} &= E(s) \, \frac{\mathrm{d}\hat{U}}{\mathrm{d}s}\Big|_{s=-1} \,. \end{aligned} \tag{6.27}$$

Applying these boundary conditions, the transfer matrix of one cell with the inhomogeneous region can be formed. Let us see how conditions (6.27) look like for cases with the positive and negative Young's modulus gradient.

6.3.1.1 Positive Linear Gradient of Young's Modulus

The one cell with the positive linear gradient of Young's modulus and the neighboring cells, where Region I has the constant Young's modulus E_{A} and Region II is also of the same type, e.g. Young's modulus changes linearly from E_{A} to E_{B}, is represented in Fig. 35.

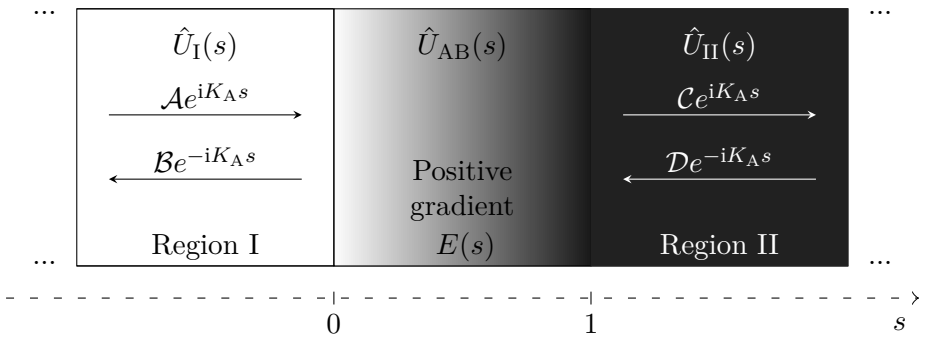

Fig. 35 Reflection and transmission of an elastic wave in a region with the positive linear gradient of the Young's Modulus.

The waves in the regions are described by the equations

$$\hat{U}_{\mathrm{I}}(s) = \mathcal{A}e^{\mathrm{i}K_{\mathrm{A}}s} + \mathcal{B}e^{-\mathrm{i}K_{\mathrm{A}}s} \,, \tag{6.28}$$

$$\hat{U}_{\mathrm{AB}}(s) = C_1 \mathrm{J}_0\left(2K_{\mathrm{A}}\frac{\sqrt{1+as}}{a}\right) + C_2 \mathrm{Y}_0\left(2K_{\mathrm{A}}\frac{\sqrt{1+as}}{a}\right) \,, \tag{6.29}$$

$$\hat{U}_{\mathrm{II}}(s) = \mathcal{C}e^{\mathrm{i}K_{\mathrm{A}}s} + \mathcal{D}e^{-\mathrm{i}K_{\mathrm{A}}s} \,. \tag{6.30}$$

Applying Eqs. (6.28) - (6.30), the boundary conditions (6.27) for the positive linear gradient, where $E(s=-1) = E_{\mathrm{B}}$, are

$$\begin{aligned}
\hat{U}_{\mathrm{I}}\Big|_{s=-0} &= \hat{U}_{AB}\Big|_{s=+0} \,, \\
\frac{\mathrm{d}\hat{U}_{\mathrm{I}}}{\mathrm{d}s}\Big|_{s=-0} &= \frac{\mathrm{d}\hat{U}_{\mathrm{AB}}}{\mathrm{d}s}\Big|_{s=+0} \,, \\
\hat{U}_{\mathrm{II}}\Big|_{s=+1} &= \hat{U}_{\mathrm{AB}}\Big|_{s=-1} \,, \\
E_{\mathrm{A}}\,\frac{\mathrm{d}\hat{U}_{\mathrm{II}}}{\mathrm{d}s}\Big|_{s=+1} &= E_{\mathrm{B}}\,\frac{\mathrm{d}\hat{U}_{\mathrm{AB}}}{\mathrm{d}s}\Big|_{s=-1} \,.
\end{aligned} \tag{6.31}$$

After the substitution of the wave equations into the system (6.31), the boundary conditions for the positive linear gradient are

$$\begin{aligned}
\mathcal{A} + \mathcal{B} &= C_1 \mathrm{J}_0\left(2K_{\mathrm{A}}\frac{1}{a}\right) + C_2 \mathrm{Y}_0\left(2K_{\mathrm{A}}\frac{1}{a}\right) \,, \\
\mathrm{i}\,(\mathcal{A} - \mathcal{B}) &= -\left[C_1 \mathrm{J}_1\left(2K_{\mathrm{A}}\frac{1}{a}\right) + C_2 \mathrm{Y}_1\left(2K_{\mathrm{A}}\frac{1}{a}\right)\right] \,, \\
\mathcal{C}e^{\mathrm{i}K_{\mathrm{A}}} + \mathcal{D}e^{-\mathrm{i}K_{\mathrm{A}}} &= C_1 \mathrm{J}_0\left(2K_{\mathrm{A}}\frac{\sqrt{1+a}}{a}\right) + C_2 \mathrm{Y}_0\left(2K_{\mathrm{A}}\frac{\sqrt{1+a}}{a}\right) \,, \\
\mathrm{i}E_{\mathrm{A}}\left(\mathcal{C}e^{\mathrm{i}K_{\mathrm{A}}} - \mathcal{D}e^{-\mathrm{i}K_{\mathrm{A}}}\right) &= -\frac{E_{\mathrm{B}}}{\sqrt{1+a}}\left[C_1 \mathrm{J}_1\left(2K_{\mathrm{A}}\frac{\sqrt{1+a}}{a}\right) + C_2 \mathrm{Y}_1\left(2K_{\mathrm{A}}\frac{\sqrt{1+a}}{a}\right)\right] \,.
\end{aligned} \tag{6.32}$$

6.3.1.2 Negative Linear Gradient of Young's Modulus

The one cell with the negative linear gradient of Young's modulus and the neighboring cells, where Region I has the constant Young's modulus E_{B} and Region II is also of the same type, e.g. Young's modulus changes linearly from E_{B} to E_{A}, is represented in Fig. 36.

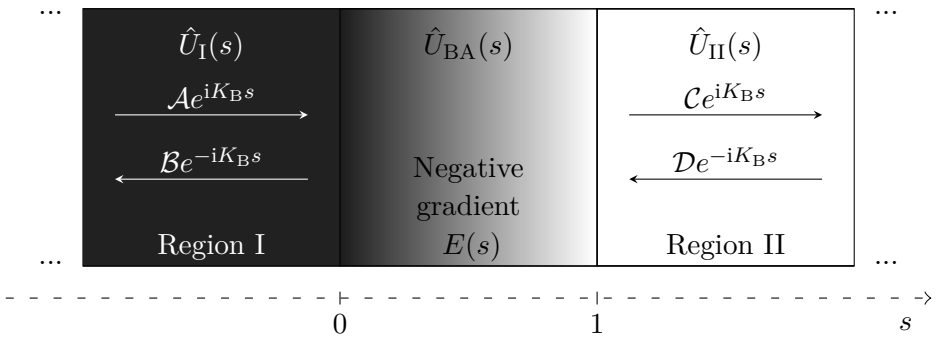

Fig. 36 Reflection and transmission of an elastic wave in a region with the negative linear gradient of the Young's Modulus.

The waves in the regions are described by the equations

$$\hat{U}_{\mathrm{I}}(s) = \mathcal{A}e^{\mathrm{i}K_{\mathrm{B}}s} + \mathcal{B}e^{-\mathrm{i}K_{\mathrm{B}}s} \,, \tag{6.33}$$

$$\hat{U}_{\mathrm{BA}}(s) = C_3 \mathrm{J}_0\left(2K_{\mathrm{B}}\frac{\sqrt{1-bs}}{b}\right) + C_4\left[\mathrm{Y}_0\left(2K_{\mathrm{B}}\frac{\sqrt{1-bs}}{b}\right) + \mathrm{i}2\mathrm{J}_0\left(2K_{\mathrm{B}}\frac{\sqrt{1-bs}}{b}\right)\right] \,, \tag{6.34}$$

$$\hat{U}_{\mathrm{II}}(s) = \mathcal{C}e^{\mathrm{i}K_{\mathrm{B}}s} + \mathcal{D}e^{-\mathrm{i}K_{\mathrm{B}}s} \,. \tag{6.35}$$

Applying Eqs. (6.33) - (6.35), the boundary conditions (6.27) for the negative linear gradient, where $E(s=-1) = E_{\mathrm{A}}$, are

$$\begin{aligned}
\hat{U}_{\mathrm{I}}\Big|_{s=-0} &= \hat{U}_{BA}\Big|_{s=+0} \,, \\
\frac{\mathrm{d}\hat{U}_{\mathrm{I}}}{\mathrm{d}s}\Big|_{s=-0} &= \frac{\mathrm{d}\hat{U}_{\mathrm{BA}}}{\mathrm{d}s}\Big|_{s=+0} \,, \\
\hat{U}_{\mathrm{II}}\Big|_{s=+1} &= \hat{U}_{\mathrm{BA}}\Big|_{s=-1} \,, \\
E_{\mathrm{B}}\,\frac{\mathrm{d}\hat{U}_{\mathrm{II}}}{\mathrm{d}s}\Big|_{s=+1} &= E_{\mathrm{A}}\,\frac{\mathrm{d}\hat{U}_{\mathrm{BA}}}{\mathrm{d}s}\Big|_{s=-1} \,.
\end{aligned} \tag{6.36}$$

After the substitution of the wave equations into the system (6.36), the boundary conditions for the negative linear gradient are

$$\begin{aligned}
\mathcal{A}+\mathcal{B} &= C_3\mathrm{J}_0\left(2K_{\mathrm{B}}\frac{1}{b}\right) + C_4\left[\mathrm{Y}_0\left(2K_{\mathrm{B}}\frac{1}{b}\right) + 2\mathrm{i}\mathrm{J}_0\left(2K_{\mathrm{B}}\frac{1}{b}\right)\right] \,, \\
\mathrm{i}\,(\mathcal{A}-\mathcal{B}) &= C_3\mathrm{J}_1\left(2K_{\mathrm{B}}\frac{1}{b}\right) + C_4\left[\mathrm{Y}_1\left(2K_{\mathrm{B}}\frac{1}{b}\right) + 2\mathrm{i}\mathrm{J}_1\left(2K_{\mathrm{B}}\frac{1}{b}\right)\right] \,, \\
\mathcal{C}e^{\mathrm{i}K_{\mathrm{B}}} + \mathcal{D}e^{-\mathrm{i}K_{\mathrm{B}}} &= C_3\mathrm{J}_0\left(2K_{\mathrm{B}}\frac{\sqrt{1-b}}{b}\right) + C_4\left[\mathrm{Y}_0\left(2K_{\mathrm{B}}\frac{\sqrt{1-b}}{b}\right) + 2\mathrm{i}\mathrm{J}_0\left(2K_{\mathrm{B}}\frac{\sqrt{1-b}}{b}\right)\right], \\
\mathrm{i}E_{\mathrm{B}}\left(\mathcal{C}e^{\mathrm{i}K_{\mathrm{B}}} - \mathcal{D}e^{-\mathrm{i}K_{\mathrm{B}}}\right) &= \frac{E_{\mathrm{A}}}{\sqrt{1-b}}\left(C_3\mathrm{J}_1\left(2K_{\mathrm{B}}\frac{\sqrt{1-b}}{b}\right) + \right. \\
&\qquad \left. C_4\left[\mathrm{Y}_1\left(2K_{\mathrm{B}}\frac{\sqrt{1-b}}{b}\right) + 2\mathrm{i}\mathrm{J}_1\left(2K_{\mathrm{B}}\frac{\sqrt{1-b}}{b}\right)\right]\right) .
\end{aligned} \tag{6.37}$$

6.3.2 Transfer Matrix

Let us write the transfer matrices $\mathbf{M}(s_b, s_a)$ and $\mathbf{P}(s_b, s_a)$ of one cell represented by an inhomogeneous region

$$\mathbf{M}(1,0) = \begin{pmatrix} w & z \\ z^* & w^* \end{pmatrix} , \tag{6.38}$$

$$\mathbf{P}(1,0) = \begin{pmatrix} we^{\mathrm{i}K} & ze^{\mathrm{i}K} \\ z^*e^{-\mathrm{i}K} & w^*e^{-\mathrm{i}K} \end{pmatrix} , \tag{6.39}$$

since the symmetry property has place.

The shifted transfer matrix differs for positive and negative gradients. The difference is in a wave number K.

6.3.2.1 Positive Linear Gradient of Young's Modulus

The shifted transfer matrix for the positive linear gradient of Young's modulus equals

$$\mathbf{P}(1,0) = \begin{pmatrix} e^{\mathrm{i}K_\mathrm{A}} & 0 \\ 0 & e^{-\mathrm{i}K_\mathrm{A}} \end{pmatrix} \mathbf{M}(1,0) = \begin{pmatrix} we^{\mathrm{i}K_\mathrm{A}} & ze^{\mathrm{i}K_\mathrm{A}} \\ z^*e^{-\mathrm{i}K_\mathrm{A}} & w^*e^{-\mathrm{i}K_\mathrm{A}} \end{pmatrix} . \tag{6.40}$$

6.3.2.2 Negative Linear Gradient of Young's Modulus

The shifted transfer matrix for the negative linear gradient of Young's modulus is

$$\mathbf{P}(1,0) = \begin{pmatrix} e^{\mathrm{i}K_\mathrm{B}} & 0 \\ 0 & e^{-\mathrm{i}K_\mathrm{B}} \end{pmatrix} \mathbf{M}(1,0) = \begin{pmatrix} we^{\mathrm{i}K_\mathrm{B}} & ze^{\mathrm{i}K_\mathrm{B}} \\ z^*e^{-\mathrm{i}K_\mathrm{B}} & w^*e^{-\mathrm{i}K_\mathrm{B}} \end{pmatrix} . \tag{6.41}$$

6.3.3 Transfer Matrix Feature

The transfer matrix of the cell describing the propagation of elastic waves through the linearly graded material has one feature separating it from the transfer matrices discussed earlier in the work: the determinant is not equal to one. This feature influences the transmission coefficient formula.

6.3.3.1 Determinant

The determinants of the transfer matrices are not equal to one generally, so the value of the one cell determinant is

$$\det \mathbf{M}(1,0) = |w|^2 - |z|^2 = \det \mathbf{P}(1,0) . \tag{6.42}$$

6.3.3.2 Transmission Coefficient

Applying the transmission coefficient formula (2.17) to one cell described by Eq. (6.38) with the non-unitary determinant leads to

$$\mathcal{T} = \frac{\det(\mathbf{M}(1,0))}{M_{22}} = \frac{\det(\mathbf{M}(1,0))}{w^*} , \tag{6.43}$$

so the modulus of the transmission coefficient (6.43), based on Eq. (2.19), is

$$|\mathcal{T}| = \left| \frac{\det(\mathbf{M}(1,0))}{w^*} \right| . \tag{6.44}$$

6.4 Multiple Cells

The construction of the solid rode consisted of N repeating cells with positive/negative gradient is analogically to the already considered cell types. The Chebyshev identity has place since the determinants are real. So it can be applied to calculate the transfer matrix of N inhomogeneous regions constituted the solid rode.

6.4.1 Transfer Matrix of N Cells

The shifted transfer matrix for N cells has the form

$$\mathbf{P}_N = \begin{pmatrix} U_N(\mu) - w^* e^{-\mathrm{i}K} U_{N-1}(\mu) & z e^{\mathrm{i}K} U_{N-1}(\mu) \\ z^* e^{-\mathrm{i}K} U_{N-1}(\mu) & U_N(\mu) - w e^{\mathrm{i}K} U_{N-1}(\mu) \end{pmatrix} . \tag{6.45}$$

The transfer matrix for N cells then is

$$\begin{aligned} \mathbf{M}_N &= \begin{pmatrix} e^{-\mathrm{i}KN} & 0 \\ 0 & e^{\mathrm{i}KN} \end{pmatrix} \mathbf{P}_N \\ &= \begin{pmatrix} e^{-\mathrm{i}KN} \left[U_N(\mu) - w^* e^{-\mathrm{i}K} U_{N-1}(\mu) \right] & z e^{-\mathrm{i}K(N-1)} U_{N-1}(\mu) \\ z^* e^{\mathrm{i}K(N-1)} U_{N-1}(\mu) & e^{\mathrm{i}KN} \left[U_N(\mu) - w e^{\mathrm{i}K} U_{N-1}(\mu) \right] \end{pmatrix} , \end{aligned} \tag{6.46}$$

where

$$\mu = \frac{1}{2} \mathrm{Tr}(\mathbf{P}(1,0)) = \frac{1}{2} \left(w e^{\mathrm{i}K} + w^* e^{-\mathrm{i}K} \right) . \tag{6.47}$$

6.4.2 Transmission Coefficient

The transmission coefficient modulus of the system of N cells, based on Eqs. (6.44) and (6.46), is

$$|\mathcal{T}_N| = \left| \frac{\det(\mathbf{M}_N)}{M_{N_{22}}} \right| = \frac{|\det(\mathbf{M}(1,0))|^N}{|U_N(\mu) - w e^{\mathrm{i}K} U_{N-1}(\mu)|} . \tag{6.48}$$

6.4.2.1 Positive Linear Gradient of Young's Modulus

The solid rode consisted of N repeating cells with positive linear gradient of Young's modulus is represented in Fig. 37.

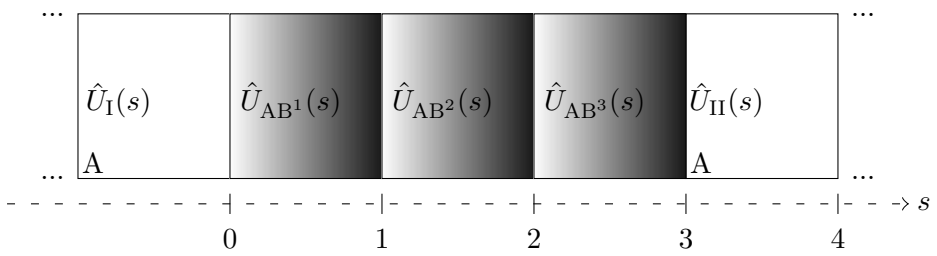

Fig. 37 Multiple cells with positive linear gradient of Young's modulus.

Using formula (6.46) the transfer matrix for this case is

$$\begin{aligned}\mathbf{M}_N &= \begin{pmatrix} e^{-\mathrm{i}K_\mathrm{A}N} & 0 \\ 0 & e^{\mathrm{i}K_\mathrm{A}N} \end{pmatrix} \mathbf{P}_N \\ &= \begin{pmatrix} e^{-\mathrm{i}K_\mathrm{A}N}\left[U_N(\mu) - w^* e^{-\mathrm{i}K_\mathrm{A}} U_{N-1}(\mu)\right] & z e^{-\mathrm{i}K_\mathrm{A}(N-1)} U_{N-1}(\mu) \\ z^* e^{\mathrm{i}K_\mathrm{A}(N-1)} U_{N-1}(\mu) & e^{\mathrm{i}K_\mathrm{A}N}\left[U_N(\mu) - w e^{\mathrm{i}K_\mathrm{A}} U_{N-1}(\mu)\right] \end{pmatrix}. \end{aligned} \tag{6.49}$$

The needed expressions are

$$\begin{aligned} w &= \frac{E_\mathrm{A}\sqrt{1+a}\alpha_1 + E_\mathrm{B}\alpha_2 + \mathrm{i}\left[E_\mathrm{A}\sqrt{1+a}\alpha_3 + E_\mathrm{B}\alpha_4\right]}{2e^{\mathrm{i}2K_\mathrm{A}} E_\mathrm{A}\sqrt{1+a}\alpha_5}\,, \\ z &= \frac{E_\mathrm{A}\sqrt{1+a}\alpha_1 - E_\mathrm{B}\alpha_2 - \mathrm{i}\left[E_\mathrm{A}\sqrt{1+a}\alpha_3 - E_\mathrm{B}\alpha_4\right]}{2e^{\mathrm{i}2K_\mathrm{A}} E_\mathrm{A}\sqrt{1+a}\alpha_5}\,, \\ \mu &= \frac{1}{2}\left(w e^{\mathrm{i}K_\mathrm{A}} + w^* e^{-\mathrm{i}K_\mathrm{A}}\right)\,, \\ \det(\mathbf{M}(1,0)) &= \frac{E_\mathrm{B}\alpha_6}{E_\mathrm{A}\sqrt{1+a}\alpha_5}\,, \end{aligned} \tag{6.50}$$

the used designations are

$$\begin{aligned} \alpha_1 &= \mathrm{J}_0(arg_a(1))\mathrm{Y}_1(arg_a(0)) - \mathrm{Y}_0(arg_a(1))\mathrm{J}_1(arg_a(0))\,, \\ \alpha_2 &= \mathrm{J}_0(arg_a(0))\mathrm{Y}_1(arg_a(1)) - \mathrm{Y}_0(arg_a(0))\mathrm{J}_1(arg_a(1))\,, \\ \alpha_3 &= \mathrm{J}_0(arg_a(1))\mathrm{Y}_0(arg_a(0)) - \mathrm{J}_0(arg_a(0))\mathrm{Y}_0(arg_a(1))\,, \\ \alpha_4 &= \mathrm{J}_1(arg_a(1))\mathrm{Y}_1(arg_a(0)) - \mathrm{J}_1(arg_a(0))\mathrm{Y}_1(arg_a(1))\,, \\ \alpha_5 &= \mathrm{J}_0(arg_a(0))\mathrm{Y}_1(arg_a(0)) - \mathrm{Y}_0(arg_a(0))\mathrm{J}_1(arg_a(0))\,, \\ \alpha_6 &= \mathrm{J}_0(arg_a(1))\mathrm{Y}_1(arg_a(1)) - \mathrm{Y}_0(arg_a(1))\mathrm{J}_1(arg_a(1))\,, \end{aligned} \tag{6.51}$$

where

$$arg_a(s) = 2K_\mathrm{A}\frac{\sqrt{1+as}}{a} = \begin{cases} arg_a(0) = 2K_\mathrm{A}\dfrac{1}{a}\,, \\ arg_a(1) = 2K_\mathrm{A}\dfrac{\sqrt{1+a}}{a}\,. \end{cases} \tag{6.52}$$

Finally, the transmission coefficient formula, based on Eq. (6.48), is

$$|\mathcal{T}_N| = \frac{|\det(\mathbf{M}(1,0))|^N}{|U_N(\mu) - w e^{\mathrm{i}K_\mathrm{A}} U_{N-1}(\mu)|}\,. \tag{6.53}$$

To achieve the band gap with the smallest possible number of cells, the difference between Young's moduli should be high. Carbon steel C $\geq$ 0.3% has been chosen as material, Young's modulus E_A is 202 GPa at 21°C and E_B = 106 GPa at 649°C (see e.g. [14]). For the chosen material and its values the bang gap is achieved for $N = 40$ cells, see Fig. 38.

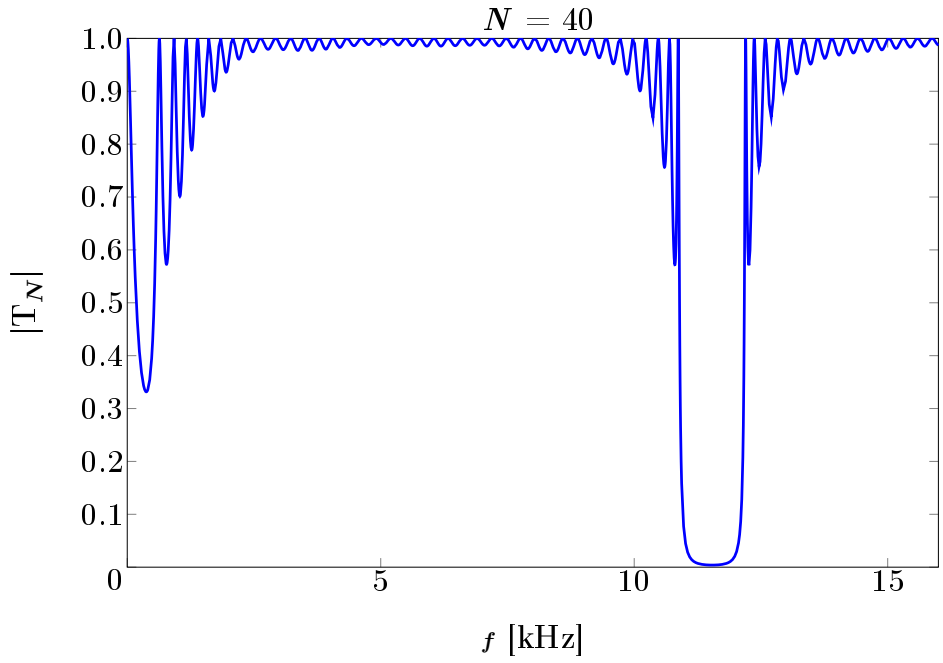

Fig. 38 Dependence of the transmission coefficient modulus on frequency for positive gradient of Young's modulus (carbon steel C $\geq 0.3\%$).

6.4.2.2 Negative Linear Gradient of Young's Modulus

The solid rode consisted of N repeating cells with negative linear gradient of Young's modulus is represented in Fig. 39.

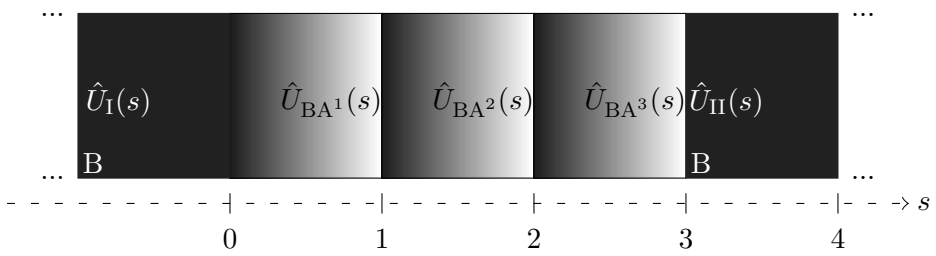

Fig. 39 Multiple cells with negative linear gradient of Young's modulus.

Using formula (6.46) the transfer matrix for this case is

$$\begin{aligned}\mathbf{M}_N &= \begin{pmatrix} e^{-\mathrm{i}K_\mathrm{B}N} & 0 \\ 0 & e^{\mathrm{i}K_\mathrm{B}N} \end{pmatrix} \mathbf{P}_N \\ &= \begin{pmatrix} e^{-\mathrm{i}K_\mathrm{B}N}\left[U_N(\mu) - w^* e^{-\mathrm{i}K_\mathrm{B}} U_{N-1}(\mu)\right] & z e^{-\mathrm{i}K_\mathrm{B}(N-1)} U_{N-1}(\mu) \\ z^* e^{\mathrm{i}K_\mathrm{B}(N-1)} U_{N-1}(\mu) & e^{\mathrm{i}K_\mathrm{B}N}\left[U_N(\mu) - w e^{\mathrm{i}K_\mathrm{B}} U_{N-1}(\mu)\right] \end{pmatrix}. \end{aligned} \quad (6.54)$$

The needed expressions are

$$\begin{aligned} w &= \frac{E_{\mathrm{B}}\sqrt{1-b}\beta_1 + E_{\mathrm{A}}\beta_2 - \mathrm{i}\left[E_{\mathrm{B}}\sqrt{1-b}\beta_3 + E_{\mathrm{A}}\beta_4\right]}{2e^{\mathrm{i}2K_{\mathrm{B}}}E_{\mathrm{B}}\sqrt{1-b}\beta_5}\ , \\ z &= \frac{E_{\mathrm{B}}\sqrt{1-b}\beta_1 - E_{\mathrm{A}}\beta_2 + \mathrm{i}\left[E_{\mathrm{B}}\sqrt{1-b}\beta_3 - E_{\mathrm{A}}\beta_4\right]}{2e^{\mathrm{i}2K_{\mathrm{B}}}E_{\mathrm{B}}\sqrt{1-b}\beta_5}\ , \\ \mu &= \frac{1}{2}\left(we^{\mathrm{i}K_{\mathrm{B}}} + w^* e^{-\mathrm{i}K_{\mathrm{B}}}\right)\ , \\ \det(\mathbf{M}(1,0)) &= \frac{E_{\mathrm{A}}\beta_6}{E_{\mathrm{B}}\sqrt{1-b}\beta_5}\ , \end{aligned} \tag{6.55}$$

the used designations are

$$\begin{aligned} \beta_1 &= \mathrm{J}_0(arg_b(1))\mathrm{Y}_1(arg_b(0)) - \mathrm{Y}_0(arg_b(1))\mathrm{J}_1(arg_b(0))\ , \\ \beta_2 &= \mathrm{J}_0(arg_b(0))\mathrm{Y}_1(arg_b(1)) - \mathrm{Y}_0(arg_b(0))\mathrm{J}_1(arg_b(1))\ , \\ \beta_3 &= \mathrm{J}_0(arg_b(1))\mathrm{Y}_0(arg_b(0)) - \mathrm{J}_0(arg_b(0))\mathrm{Y}_0(arg_b(1))\ , \\ \beta_4 &= \mathrm{J}_1(arg_b(1))\mathrm{Y}_1(arg_b(0)) - \mathrm{J}_1(arg_b(0))\mathrm{Y}_1(arg_b(1))\ , \\ \beta_5 &= \mathrm{J}_0(arg_b(0))\mathrm{Y}_1(arg_b(0)) - \mathrm{Y}_0(arg_b(0))\mathrm{J}_1(arg_b(0))\ , \\ \beta_6 &= \mathrm{J}_0(arg_b(1))\mathrm{Y}_1(arg_b(1)) - \mathrm{Y}_0(arg_b(1))\mathrm{J}_1(arg_b(1))\ , \end{aligned} \tag{6.56}$$

where

$$arg_b(s) = 2K_{\mathrm{B}}\frac{\sqrt{1-bs}}{b} = \begin{cases} arg_b(0) = 2K_{\mathrm{B}}\dfrac{1}{b}\ , \\ arg_b(1) = 2K_{\mathrm{B}}\dfrac{\sqrt{1-b}}{b}\ . \end{cases} \tag{6.57}$$

Finally, the transmission coefficient formula, based on Eq. (6.48), is

$$|\mathcal{T}_N| = \frac{|\det(\mathbf{M}(1,0))|^N}{|U_N(\mu) - we^{\mathrm{i}K_{\mathrm{B}}}U_{N-1}(\mu)|}\ . \tag{6.58}$$

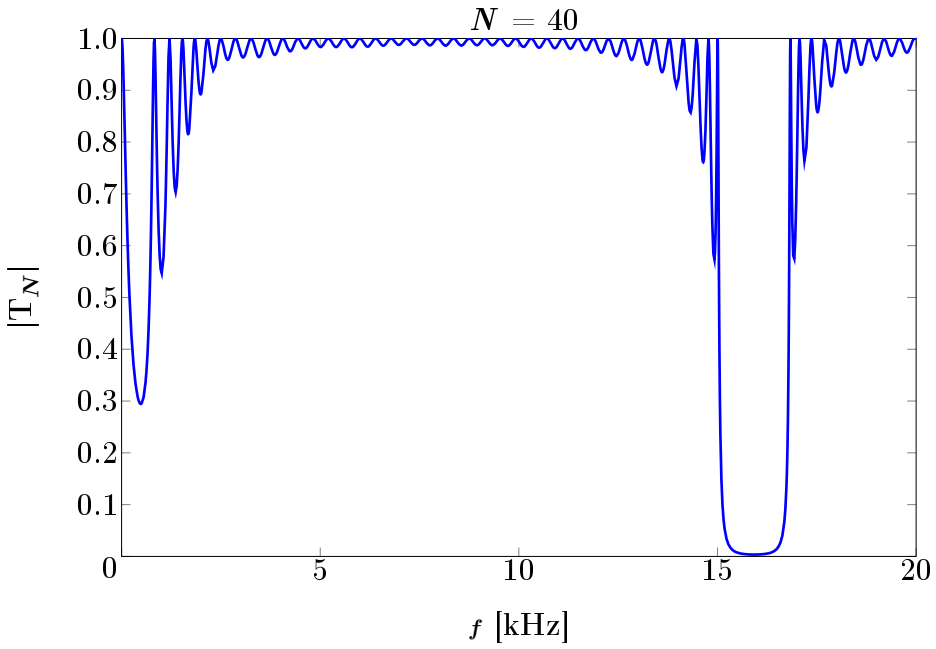

Fig. 40 Dependence of the transmission coefficient modulus on frequency for positive gradient of Young's modulus (carbon steel C $\geq$ 0.3%).

The band gap for the negative gradient has also place for $N = 40$ cells, this occurrence is represented in Fig. 40. Comparing the results for the positive and negative gradients can be concluded that for the negative gradient the band gap occurs at higher frequencies than for the positive one. For the negative gradient the band gap is wider than for the positive gradient.

6.4.2.3 Triangular Profile of Young's Modulus Gradient

Let us combine the positive and negative gradients of Young's Modulus. The solid rode consisted of N repeating cells of this kind is represented in Fig. 41.

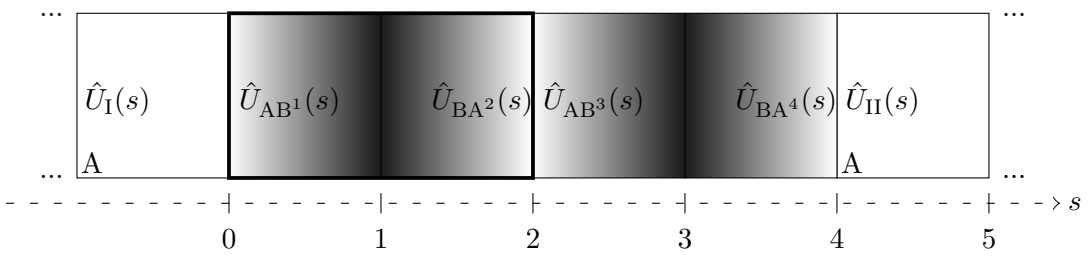

Fig. 41 Multiple cells with positive linear gradient of Young's modulus.

Since the transfer matrices for positive and negative gradients have already been derived, the transfer matrix of the combination of these gradients, represented the cell, can be easily written down. Let us call this type of the cell as a *triangular* profile of Young's modulus (see e.g. [15]). In order to distinguish the elements of the transfer matrices, let the elements w_1 and z_1 be the elements in case of the positive gradient, w_2 and z_2 are of negative one.

One cell, as it can be seen in Fig. 41, is from 0 to 2. The shifted transfer matrix of one cell is

$$\begin{aligned}\mathbf{P}(2,0) &= \begin{pmatrix} e^{\mathrm{i}(K_{\mathrm{A}}+2K_{\mathrm{B}})} & 0 \\ 0 & e^{-\mathrm{i}(K_{\mathrm{A}}+2K_{\mathrm{B}})} \end{pmatrix} \mathbf{M}_{neg}(1,0)\mathbf{M}_{pos}(1,0) \\ &= \begin{pmatrix} e^{\mathrm{i}(K_{\mathrm{A}}+2K_{\mathrm{B}})} & 0 \\ 0 & e^{-\mathrm{i}(K_{\mathrm{A}}+2K_{\mathrm{B}})} \end{pmatrix} \begin{pmatrix} w & z \\ z^* & w^* \end{pmatrix} , \end{aligned} \tag{6.59}$$

where

$$\begin{aligned} w &= w_2 w_1 + z_2 z_1^* , \\ z &= w_2 z_1 + z_2 w_1^* , \\ \mu &= \frac{1}{2}\left(w e^{\mathrm{i}(K_{\mathrm{A}}+2K_{\mathrm{B}})} + w^* e^{-\mathrm{i}(K_{\mathrm{A}}+2K_{\mathrm{B}})} \right) . \end{aligned} \tag{6.60}$$

The determinant is

$$\det(\mathbf{P}(2,0)) = \det(\mathbf{M}(2,0)) = \frac{\alpha_6\beta_6}{\sqrt{1+a}\sqrt{1-b}\alpha_5\beta_5} = 1 . \tag{6.61}$$

So, the transfer matrix determinant is unimodular, because the cell has the symmetry.

The transfer matrix for N cells is

$$\begin{aligned}\mathbf{M}_N &= \begin{pmatrix} e^{-\mathrm{i}(K_{\mathrm{A}}+2K_{\mathrm{B}})N} & 0 \\ 0 & e^{\mathrm{i}(K_{\mathrm{A}}+2K_{\mathrm{B}})N} \end{pmatrix} \mathbf{P}_N \\ &= \begin{pmatrix} e^{-\mathrm{i}KN}\left[U_N(\mu) - w^* e^{-\mathrm{i}K} U_{N-1}(\mu)\right] & z e^{-\mathrm{i}K(N-1)} U_{N-1}(\mu) \\ z^* e^{\mathrm{i}K(N-1)} U_{N-1}(\mu) & e^{\mathrm{i}KN}\left[U_N(\mu) - w e^{\mathrm{i}K} U_{N-1}(\mu)\right] \end{pmatrix} , \end{aligned} \tag{6.62}$$

where

$$K = K_{\mathrm{A}} + 2K_{\mathrm{B}} \ . \tag{6.63}$$

The transmission coefficient modulus is

$$|\mathcal{T}_N| = \frac{1}{|\ U_N(\mu) - we^{\mathrm{i}K} U_{N-1}(\mu)\ |} \ . \tag{6.64}$$

The band gap for the triangle profile of Young's modulus has already place for $N = 35$ cells, this occurrence is represented in Fig. 42. In comparison to the positive and negative gradients taken separately the chosen combination of gradients shifts the band gap to the low frequencies. Moreover, there are three band gaps at lower frequencies than in a case of the positive gradient.

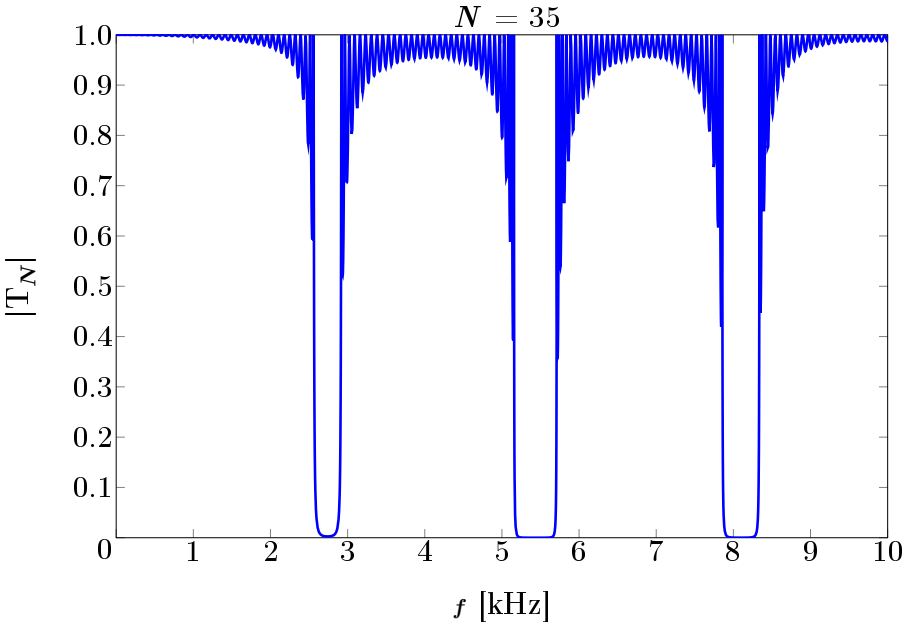

Fig. 42 Dependence of the transmission coefficient modulus on frequency for triangle profile of Young's modulus (carbon steel C $\geq$ 0.3%).

7 Conclusion

In this master thesis, the propagation of the longitudinal elastic waves through the locally periodic structures excited by a harmonic force have been studied. The frequency band gaps were the main object of interest. The material of the locally periodic structures (one-dimensional phononic crystals) had non-uniform profile of the mass density and elastic parameters or non-uniform profile of the cross-section only. The corresponding model equation was derived. Different types of the cells constituting the solid rod were considered. Dispersion zones were taken as spatially bounded regions with the functionally changing material properties. The transfer matrix method have been applied to study the elastic waves passing through the inhomogeneous domain. The transfer matrices calculation was done through the evaluation of the general solution in the interval containing two regular singular points (boundary conditions). There were considered three cell types in the thesis: with the non-uniform cross-sections, with the non-uniform mass densities and Young's moduli and, finally, functionally graded materials, based on the linear change of Young's modulus. For the two first types were shown that by having the big ratios of the non-uniform parameter values the band gap occurrence could be already achieved for the small number of cells, e.g. just for $N = 2$ in case of the non-uniform cross-sections. It was shown that the choice of the material and geometrical parameter values influences the band gap range and amplitude, the influence of the order of the non-uniform parameter values also was represented. The known length ratio of non-uniform parts has been also considered. It was shown that this knowledge was very helpful in forming the band gaps. For the third type of the cell, where the linear gradient of Young's modulus was considered, the solution of the inhomogeneous region was represented by Bessel functions. Triangular profile has shifted the band gap to lower frequencies in comparison to the cases of just one linear gradient of Young's modulus. The transmission coefficient calculation of the locally periodic structures for N repeating cells was calculated with the help of the Chebyshev polynomials. In the studies [1], [2], [5], [6] the Chebyshev polynomials were applied to unimodular matrices, in the thesis the Chebyshev polynomials were applied for the non-unimodular matrices also.

Due to isomorphism of model equations that can be encountered in various areas of wave physics, the presented results in this work will find wider application (see e.g. [1]).

The whole work was done analytically. The calculations were made in Maple software. The assignment task has been accomplished.

Bibliography

[1] David J. Griffiths and Carl A. Steinke. "Waves in locally periodic media". In: *Am. J. Phys.* 69.2 (2001).

[2] Peter Markoš and Costas M. Soukoulis. *Wave Propagation - From Electrons to Photonic Crystals and Left-Handed Materials*. Princeton University Press, 2008.

[3] Mario N. Armenise et al. "Phononic and photonic band gap structures: modelling and applications". In: *Physics Procedia* 3 (2010), pp. 357–364.

[4] T. Gorishnyy et al. "Sound ideas". In: *Physics World* 18 (2005), pp. 24–30.

[5] P. Pereyra. *Undergraduate Lecture Notes in Physics*. Springer, 2012.

[6] Zhuangqi Cao and Cheng Yin. *Advances in One-Dimensional Wave Mechanics*. Springer, 2014.

[7] K.F. Graff. *Wave motion in Elastic Solids*. ISBN-10: 0486667456. Dover Publications, 1975.

[8] K. Hornišová and P. Billik. "Some properties of horn equation model of ultrasonic system vibration and of transfer matrix and equivalent circuit methods of its solution". In: *Ultrasonics* 54 (2014), pp. 330–342.

[9] Rudenko O. V. and Shvartsburg A. B. "Nonlinear and Linear Wave Phenomena in Narrow Pipes". In: *Acoustical Physics* **56**.4 (2010), pp. 429–434.

[10] Payton RG. "Elastic wave propagation in a non-homogeneous rod". In: *The Quarterly Journal of Mechanics and Applied Mathematics* 19 (1966), pp. 83–91.

[11] S. H. Arshad, M. N. Naeem, and N. Sultana. "Frequency analysis of functionally graded material cylindrical shells with various volume fraction laws". In: *Journal of Mechanical Engineering Science* 221 (2007), pp. 1483–1495.

[12] *J — Bessel function of the first kind*. Nov. 1, 2017. URL: `http://www.librow.com/articles/article-11/appendix-a-34`.

[13] *Y — Bessel function of the second kind*. Nov. 1, 2017. URL: `http://www.librow.com/articles/article-11/appendix-a-35`.

[14] *Young's Modulus of Elasticity for Metals and Alloys*. Nov. 13, 2017. URL: `https://www.engineeringtoolbox.com/young-modulus-d_773.html`.

[15] G. V. Morozov, D. W. L. Sprung, and J. Martorell. "One-dimensional photonic crystals with a sawtooth refractive index: another exactly solvable potential". In: *New Journal of Physics* 15 (2013).

Appendix A

Attached CD contents

Maple calculation worksheets. These worksheets contain all calculations and graphs represented in the thesis. The worksheets are organized according to the chapters.
Electronic version of the thesis in PDF.